AD-A176 851 EXPERIMENTAL AND THEORETICAL STUDIES OF LASER PROPULSION PHENOMENOLOGY(U) PHYSICAL SCIENCES INC ANDOVER MA D ROSEN ET AL. 10 DEC 86 PSI-034/TR-579 1/1

UNCLASSIFIED AFOSR-TR-87-0125 F49620-85-C-0072 F/G 21/8 NL

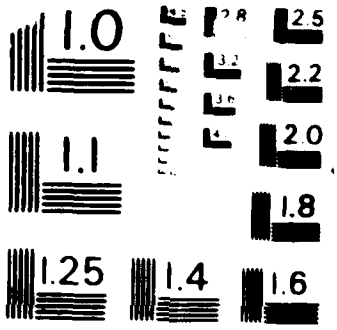
1.0
2.8
2.5
3.2
2.2
3.6
2.0
4
1.1
1.8
1.25
1.4
1.6

AD-A176 851

AFOSR-TR- 87-0125

DTIC
ELECTE
FEB 19 1987
S D
D

PSI-034/TR-579

EXPERIMENTAL AND THEORETICAL STUDIES OF LASER PROPULSION PHENOMENOLOGY

[illegible] release;
[illegible] unlimited.

D. Rosen, N. Kemp, R. Krech,
J. Campbell, and G. Caledonia
Physical Sciences Inc.
P.O. Box 3100
Andover, MA 01810

[illegible] (AFSC)

18 December 1986

Final Technical Report

Prepared for

AIR FORCE OFFICE OF SCIENTIFIC RESEARCH (AFSC)
Bolling Air Force Base
Washington, DC 20332

87 2 [illegible] 130

UNCLASSIFIED

SECURITY CLASSIFICATION OF THIS PAGE

ADA176851

REPORT DOCUMENTATION PAGE

1a. REPORT SECURITY CLASSIFICATION Unclassified	1b. RESTRICTIVE MARKINGS None
2a. SECURITY CLASSIFICATION AUTHORITY	3. DISTRIBUTION/AVAILABILITY OF REPORT Distribution unlimited; Approved for release
2b. DECLASSIFICATION/DOWNGRADING SCHEDULE	
4. PERFORMING ORGANIZATION REPORT NUMBER(S) TR-579/PSI-034	5. MONITORING ORGANIZATION REPORT NUMBER(S) AFOSR-TR- 87-0125
6a. NAME OF PERFORMING ORGANIZATION Physical Sciences Inc. 6b. OFFICE SYMBOL (If applicable)	7a. NAME OF MONITORING ORGANIZATION Air Force Office of Scientific Research
6c. ADDRESS (City, State and ZIP Code) P.O. Box 3100 Andover, MA 01810	7b. ADDRESS (City, State and ZIP Code) Bolling Air Force Base, DC 20332-6448
8a. NAME OF FUNDING/SPONSORING ORGANIZATION same as 7a. 8b. OFFICE SYMBOL (If applicable) AFOSR/NA	9. PROCUREMENT INSTRUMENT IDENTIFICATION NUMBER F49620-85-C-0072
8c. ADDRESS (City, State and ZIP Code) same as 7b.	10. SOURCE OF FUNDING NOS. PROGRAM ELEMENT NO.: 61102F PROJECT NO.: 2308 TASK NO.: A1 WORK UNIT NO.:
11. TITLE (Include Security Classification) Experimental & Theoretical Studies of Laser Propulsion Phenomenology	
12. PERSONAL AUTHOR(S) D. Rosen, N. Kemp, R. Krech, J. Campbell, and G. Caledonia	
13a. TYPE OF REPORT Final Technical 13b. TIME COVERED FROM 4/85 TO 5/86	14. DATE OF REPORT (Yr., Mo., Day) 18 December 1986 15. PAGE COUNT 76
16. SUPPLEMENTARY NOTATION	

17. COSATI CODES			18. SUBJECT TERMS (Continue on reverse if necessary and identify by block number)
FIELD	GROUP	SUB. GR.	Propulsion, Pulsed Lasers, Thrusters, CW Lasers, Molecular Absorption, Pulse Jets
21	08		
20	13		

19. ABSTRACT (Continue on reverse if necessary and identify by block number)

This report describes a research effort carried out to provide data crucial to the ultimate development of both CW and pulsed laser propulsion technologies. The CW effort involved extending our examination of absorption of 10 and 3 μm laser radiation by molecules at elevated temperatures. Test gases were heated to temperatures of 1000 to 4500 K via shock excitation. Both absorption coefficients and saturation intensity levels were evaluated. Until these recent efforts, such a high temperature data base was virtually nonexistent and further, with the exception of diatomics, not readily amenable to theoretical extrapolation. These measurements are essential in evaluating CW laser thruster performance and, as fallout, could also provide a useful testbed for future theoretical predictions of molecular structure.

20. DISTRIBUTION/AVAILABILITY OF ABSTRACT UNCLASSIFIED/UNLIMITED ☒ SAME AS RPT. ☐ DTIC USERS ☐	21. ABSTRACT SECURITY CLASSIFICATION Unclassified
22a. NAME OF RESPONSIBLE INDIVIDUAL Dr. Julian Tishkoff	22b. TELEPHONE NUMBER (Include Area Code) (202) 767-4935 22c. OFFICE SYMBOL AFOSR/NA

DD FORM 1473, 83 APR EDITION OF 1 JAN 73 IS OBSOLETE.

UNCLASSIFIED

SECURITY CLASSIFICATION OF THIS PAGE

19. Abstract (Continued)

Pulsed laser propulsion utilizes laser-induced breakdown to develop a high temperature plasma which can subsequently be expanded to provide thrust. The three principal stages of the operation of such a thruster are: (1) laser-induced breakdown, (2) subsequent laser energy absorption in the laser-produced plasma, and (3) non-steady expansion of this hot, high pressure gas down a nozzle to produce thrust. Past studies have been devoted to characterizing the physical processes which occur in stages (1) and (2) when a high energy, short wavelength ($\lambda < 1\mu$) pulsed laser is used as the energy source. In the current effort, attention has been directed toward characterizing the final stage of the thrusting sequence. The research was carried out by utilizing and, as necessary, extending PSI's theoretical model of pulsed laser propulsion flow and laser energy absorption. The model was used to simulate previously performed laboratory experiments and the calculations compared to available data. The importance of radiation losses and non-equilibrium relaxation phenomena are also assessed.

CONTENTS

			Page
Paragraph	1	INTRODUCTION	1
	1.1	Research Related CW to Laser Propulsion	1
	1.2	Research Related to Pulsed Laser Propulsion	4
	2	STATUS OF RESEARCH EFFORT	8
	2.1	Laser Absorption by Hot Gases for CW Laser Propulsion	8
	2.1.1	CO_2 laser absorption in $H_2O/NH_3/H_2$ (Ar) mixtures	9
	2.1.2	HF laser absorption by $SF_6/H_2/Ar$ mixture	9
	2.1.3	Summary of the experimental shock tube measurements	11
	2.2	Pulsed Thruster Modeling	13
	3	WRITTEN PUBLICATIONS IN TECHNICAL JOURNALS	23
	4	LIST OF PROFESSIONAL PERSONNEL ASSOCIATED WITH RESEARCH EFFORT	24
	5	INTERACTIONS (COUPLING ACTIVITIES)	25
		REFERENCES	26
		APPENDICES	27

Accesion For
NTIS CRA&I ☑
DTIC TAB ☐
Unannounced ☐
Justification
By
Distribution /
Availability Codes
Dist | Avail and/or Special
A-1

DTIC COPY INSPECTED 6

FIGURES

			Page
FIGURE	1.	Scientific approach to research on molecular absorption for CW laser-heated thruster	3
	2.	Different states in pulsed laser thruster. (Sequence a-d is repeated after initial gas has expanded out to nozzle and fresh gas enters.)	5
	3.	Absorption of $NH_3/H_2O,H_2/Ar$ mixture at 10.6 μm . . .	10
	4.	Absorption coefficient of HF versus temperature . . .	12
	5.	Calculated specific impulse for a pulsed laser-heated thruster with hydrogen propellant. Abscissa is the laser energy deposited per unit mass in the nozzle	16
	6.	Total energy fluence profiles at various times. Hydrogen propellant. 0.53 g/s (10 atm) fill rate. 3.25J of laser energy deposited in 1.46 cm of nozzle gas. Nozzle filled for 20 μs (up to 5.6 cm)	19
	7.	Kinetic energy fluence profiles at various times. Conditions as given in Figure 6	20
	8.	Dissociation and ionization energy fluence profiles at various times. Conditions as given in Figure 6	21

1. INTRODUCTION/RESEARCH OBJECTIVES

Physical Sciences Inc. (PSI) is currently completing its third year of a program of studies for the Air Force Office of Scientific Research, Directorate of Aerospace Sciences, the objective of which has been the experimental and theoretical investigation of laser propulsion phenomenology. The overall research program has been directed toward resolving technical issues critical to the ultimate development of both continuous wave (CW) and repetitively pulsed (RP) laser propulsion devices. The research has also provided fundamental data useful for expanding the state of knowledge of the high temperature thermal and radiative behavior of selected gases. Below we provide a brief review of the program of studies and its rationale.

1.1 RESEARCH RELATED CW TO LASER PROPULSION

The physical processes involved in heating the working fluid of a rocket engine with a high power CW laser beam can be simply described. The gas is injected into the stagnation/absorption zone at a temperature most probably determined by regenerative cooling requirements. As the gas flows toward the throat it is heated by absorption of laser radiation. With hydrogen as the primary propellant constituent, the equivalent of nine 10.6 μm photons per molecule must be absorbed to reach a stagnation condition that yields a specific impulse of ~1000s.

The absorption scheme originally considered required the laser-induced breakdown of the H_2 "fuel" followed by the formation of a stable laser-supported combustion (LSC) wave. The principal absorption mechanism in this case is inverse electron bremsstrahlung which requires significant ionization levels in the gas. For pure H_2, ionization becomes significant at ~10,000 K with the development of a stable LSC wave requiring temperatures of ~20,000 K. It has been suggested that the introduction of alkali seeds, which will begin to thermally ionize at temperatures of ~3000 to 3500 K, would allow operation at temperatures of <10,000 K, thus providing a less severe thermal environment for thruster design. It is not clear that stable LSC waves can be formed at such low temperatures, however.

Although the use of alkali seeds appears promising, an LSC wave mechanism is required to heat the gas to T ~3000 to 3500 K to initiate alkali ionization. Alternatively, other "seed" molecules can absorb the laser radiation via vibration-rotation band transitions. Such absorbing molecules can provide for gas heating to temperatures of ~3000 to 3500 K, so that heating from the initially "cold" gas to stagnation conditions can be continuous rather than through laser-induced breakdown. Furthermore if such species can absorb to T ≈ 4500-5000 K, then specific impulses of 1000 to 2000s can be achieved without the need for ionization (and thus alkali seeds).

The high resolution absorption properties of potential absorbers for this approach are not well defined at temperatures exceeding 1000 K. Indeed, important absorption paths at elevated temperatures may well involve hot band transitions which cannot be adequately probed at room temperature. Furthermore most molecules will dissociate in the temperature range of interest. Finally, it is not known to what extent saturation effects will limit absorption at high irradiance levels, i.e., 10^3 to 10^6 W/cm^2.

In the research performed to date,[1,2] the investigations began with a review of potential "high" temperature molecular absorbers for CO_2 (10.6 μm), HF (2.7 μm), and DF (3.8 μm) laser radiation. Review criteria included absorption coefficient of parent molecules and dissociation fragments, ease of handling, thermodynamic stability and molecular weight. Following this initial review, measurements were obtained for the low irradiance absorption coefficients of a few of the more promising absorber candidates and their dissociation fragments. These measurements were performed in a shock tube using CO_2 laser probes and spanning the temperature range of 1000 to 4500 K. Candidate molecular species investigated thus far have included H_2O, CO_2, NH_3, SF_6 and NF_3. In the most recent efforts, saturation effects at high incident flux (10^3 to 10^6 W/cm^2) have been explored.

Figure 1 summarizes the overall scientific approach to the above described research effort. An example of the results obtained can be found in Figures 3, 4 of Section 2.

INFRARED LASER ENERGY ABSORPTION BY SEED MOLECULES
IN WORKING FLUID OF CW THRUSTERS

- ISSUES
  - OVERLAP OF LASER TRANSITIONS WITH RESONANT V-R TRANSITIONS IN MOLECULES
  - CONTRIBUTIONS OF 'HOT BAND' TRANSITIONS AT ELEVATED TEMPERATURES
  - POSSIBLE SATURATION OR BLEACHING EFFECTS AT HIGH IRRADIANCE ($10^3 \rightarrow 10^6$ W/cm^2)
  - STABILITY OF ABSORBING SPECIES AT HIGH TEMPERATURE (T > 3500 K);
    => DETAILED DISSOCIATION KINETICS MAY BE IMPORTANT
- APPROACH
  - REVIEW AND SCREEN POTENTIAL CANDIDATES FOR ABSORPTION OF CO_2 (~10 μm) AND DF (~4 μm) LASER RADIATION
  - ASSESS HIGH TEMPERATURE ABSORPTION BEHAVIOR THROUGH LASER ABSORPTION MEASUREMENTS IN SHOCK-HEATED MIXTURES OF INTEREST
  - ASSESS ABSORPTION "SATURATION" BEHAVIOR AT HIGH FLUX (10^3 - 10^6 W/cm^2) USING LABORATORY SCALE PULSED PROBE LASERS
  - UTILIZE EXPERIMENTAL RESULTS TO DEVELOP ABSORPTION ALGORITHMS

W-59

Figure 1. Scientific approach to research on molecular absorption scheme for CW laser-heated thruster.

The current year effort has involved two tasks. The first was to perform final measurements of the absorption coefficients for CO_2 laser radiation in shock-heated mixtures of $NH_3/H_2O/H_2/Ar$. These measurements were needed to establish the role of H_2 in defining the non-equilibrium absorption coefficient. The second task was to complete the measurements of HF ($\lambda \approx 2.8\mu$) laser absorption and saturation in candidate mixtures such as $H_2O/H_2/Ar$ and $SF_6/H_2/Ar$ over the temperature range of 300 to 3500 K. Now completed, the measurements can be coupled to an appropriate kinetic analysis in order to develop absorption algorithms applicable to realistic thruster conditions.

1.2 RESEARCH RELEATED TO PULSED LASER PROPULSION

In RP (repetitively-pulsed) laser propulsion the propellant energy is supplied by the absorption of short, repetitive laser pulses beamed to the thruster from a remote laser power station. In the RP thruster concept shown in Figure 2 parabolic nozzle walls focus the incoming beam to yield propellant breakdown at the focal point of this parabola. Depicted schematically in Figures 2a to 2d are the four principal stages in the operation of the pulsed laser-heated thruster: (a) ignition/breakdown, (b) post-breakdown plasma absorption and growth under the influence of the laser radiation field, (c) blast wave propagation into the surrounding gas, and (d) late-time expansion and cooling of the laser-heated gas.

In the first year of the present program we performed experimental and theoretical investigations of laser-induced gas breakdown at short laser wavelengths ($< 1\ \mu m$) for a variety of propellant gas candidates.[1] The results of those studies have helped to establish the threshold irradiances required to initiate an optically absorbing plasma and the scaling of those irradiances with gas density, pulse duration, and concentration of low ionization potential additives. With the ignition/breakdown criteria thus established, the next step was to evaluate the subsequent laser energy deposition that occurs in the post-breakdown plasma.

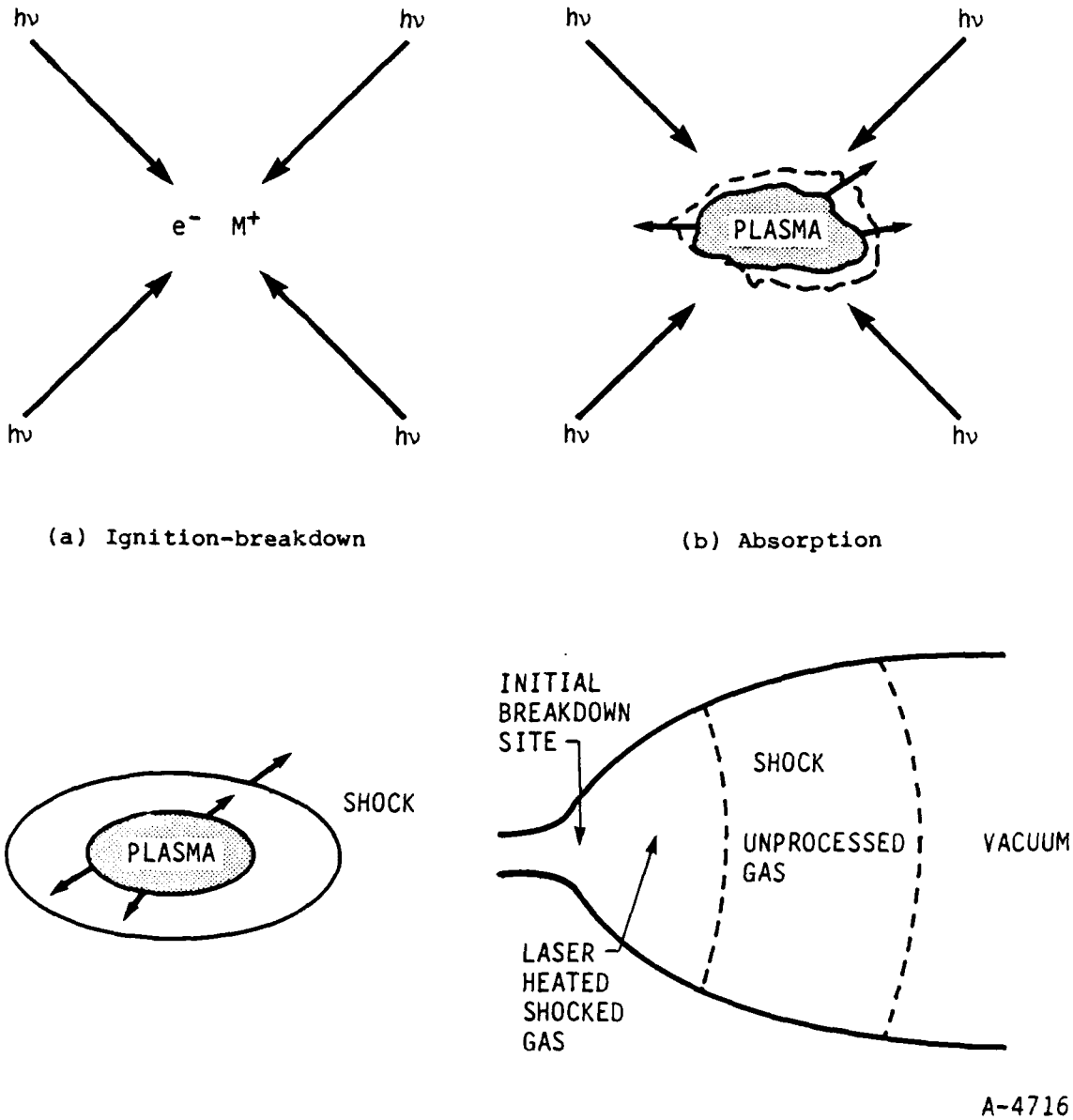

Figure 2. Different stages in pulsed laser thruster. (Sequence a-d is repeated after initial gas has expanded out of nozzle and fresh gas enters.)

In the second year research effort,[2] we performed experiments to investigate the degree of laser optical absorption and resulting plasma-dynamics which occurs when high energy pulses of 1.05 μm laser radiation are focused into various gases at focal intensities above the breakdown threshold (10^{10} to 10^{13} W/cm^2). The extent of laser energy absorption into the gas was determined from a combination of optical measurements of the laser beam attenuation by the plasma and shock trajectory measurements to infer the energy deposited in the resultant blast wave. The results indicate that, under appropriately chosen conditions, conversion efficiencies of pulsed laser energy to blast wave energy can be achieved that approach 100 percent. The data analysis also reveals, however, that a proper treatment of 'real gas' effects, i.e., energy partitioning into internal degrees of freedom of the gas, is essential to any modeling analysis.

Having carried out investigations to characterize the laser energy absorption process (Stages (a) and (b) in Figure 2) and the dynamics of the resulting blast wave (Stage (c)), the final step was to investigate the characteristics of the late time expansion (Stage (d) in Figure 2). This is the phase during which the hot, high pressure gas that is created in the upstream region of the nozzle expands, cools, and accelerates down the nozzle to produce thrust. The efficiency of this process depends on how effectively energy stored in non-thermal degrees of freedom, i.e., ionization energy, dissociation energy, etc., can be relaxed and converted to thermal (translational) energy and, ultimately, to kinetic energy directed out the nozzle exhaust.

Our knowledge about the non-steady expansion process which produces this conversion is at present uncertain. It has not yet been demonstrated that we can reliably predict the thrust or specific impulse of pulsed-laser heated thrusters. This lack of a validated predictive capability constitutes a barrier to serious consideration of this form of advanced propulsion.

However, the tools to begin validation of a prediction capability are at hand, having been developed at PSI. These tools encompass both experimental results[3] and a computer-based model.[3,4] They appear to be unique to PSI. As

far as is known, no other experiments on pulsed laser propulsion in nozzles have been performed, and no other model of the flow in such a device is available.

Experiments were performed at PSI with a 10.6 μm laser in conical and parabolic nozzles. Thrust and I_{sp} were measured on a ballistic pendulum or inferred from pressure pulse measurements in the nozzle. Concurrently, a non-steady, quasi-one-dimensional model of the laser heating and expansion process was developed at PSI. It includes equilibrium real gas effects, laser absorption, and the presence of LSD and shock waves. (It does not yet include, however, radiation from the hot gas, or non-equilibrium chemistry.)

This model, and the experimental results, have been used together to test our understanding of the nonsteady expansion process, and to decide if effects not yet included in the model play an important part in the process. Detailed calculations with the model have been compared with the experimental results to see if the model is capable of predicting them. At the same time, estimates of the effects of radiation and non-equilibrium chemistry have been made to see if they could be important in determining the results of the expansion.

Only through such comparisons will we finally know whether our ability to understand and predict the thrust performance of pulsed-laser-heated flows is at present satisfactory, or if it needs improvement. The estimates of effects not yet included in the model can be used to guide the improvements which may be needed. Such work should carry us a long way to providing convincing proof that pulsed laser propulsion can produce the combination of high thrust and high I_{sp} which is the unique property of laser-propelled rockets.

2. STATUS OF RESEARCH EFFORT

2.1 LASER ABSORPTION BY HOT GASES FOR CW LASER PROPULSION

The concept of using energy, beamed from a remote laser station, to power a rocket engine is attractive since high specific impulse can be obtained at high thrust levels.[5-9] The physical processes are simply described by a direct high pressure gas phase absorption of the laser energy in a stagnation chamber followed by a supersonic expansion of the heated gas through a nozzle. If the energy equivalent of nine 10.6 μm photons per molecule are absorbed into a propellant mixture composed primarily of hydrogen, then stagnation temperatures in excess of 4000 K can be obtained to yield a specific impulse of approximately 1000s.

Pure hydrogen can absorb IR laser radiation, but only at extremely high temperature (>10,000 K), which would create a very harsh environment in the stagnation chamber. Alternative seed molecules absorbers with an optical transition at the laser wavelength can be used to heat hydrogen via collisional energy transfer from the injection temperature to temperatures in excess of 3500 K.[7]

In previous years of this program we have studied the absorption properties of many potential molecular absorbers at CO_2 (10.6 μm) laser wavelengths.[1,2] During the past year we have performed similar measurements with mixtures of the best absorbers at 10.6 μm, and conducted other studies at HF (2.7 to 3.0 μm) wavelengths on hot HF. As in prior years these measurements were performed behind incident and reflective shock waves in the PSI 1.5 in. shock tube, under temperatures and pressure conditions which are appropriate to CW laser-heated rocket thruster operations. The apparatus used for these experiments is described in our two most recent publications which are attached as Appendix A and B, and will not be discussed in detail here. The results of our most recent CO_2 and HF measurements are discussed in the following two subsections.

2.1.1 CO_2 laser absorption in $H_2O/NH_3/H_2$ (Ar) mixtures--Our previous results indicated that NH_3 would be the absorber of choice below 2500 K and H_2O is best above 3000 K. The present study measures the absorption properties of a mixture of 4%NH_3/10%H_2O/25% H_2/Ar over a temperature range of ~750 to 3500 K. The results are presented in Figure 3, and include absorption coefficients obtained at low irradiances (~10 mW/cm^2) and high irradiances (~10^5 W/cm^2) for the mixture expressed in terms of ama^{-1} cm^{-1} for the mix of absorbers. Shown below is the anticipated absorption coefficients of the individual components NH_3 and H_2O adjusted to the mix composition. Two conclusions may be drawn. The first is that the absorption reflects the sum of the individual components within the accuracy of the measurements, and second, that no significant saturation effects are observed. Neither result is very surprising. At temperatures below 2000 K, the absorption is due primarily to NH_3, above 3000 K the absorption is due primarily to the H_2O. In the intermediate region the absorption is due to the sum of the absorption of the NH_3 and H_2O. Depending on the initial composition and temperature pressure history, the NH_3 will begin to decompose between 2000 and 3000 K. In this region the absorption is due to H_2O and some fraction of the initial NH_3 composition. Since saturation effects are not observed in either the NH_3/H_2/Ar or H_2O/H_2/Ar tests, the lack of saturation effects in mixtures of the two is not surprising.

The conclusions to be drawn from these measurements are that $NH_3/H_2O/H_2$ propellant mixtures can be employed at 10.6 μm in a CW laser heated rocket thruster to attain temperatures in excess of 3500 K to obtain specific impulses in excess of 1000s.

2.1.2 HF laser absorption by SF_6/H_2/Ar mixture--Our initial objective was to perform absorption measurements on DF laser wavelengths with D_2O. Unfortunately the pulsed DF laser output could not be made sufficiently stable to yield statistically valid absorption coefficient measurements for the allowable D_2O loading (15 torr maximum). The same was also true for H_2O at pulsed HF laser wavelengths. This is due to the fact that the laser output is slightly lower in pulsed DF and HF operation than when operated in CO_2 and the output is

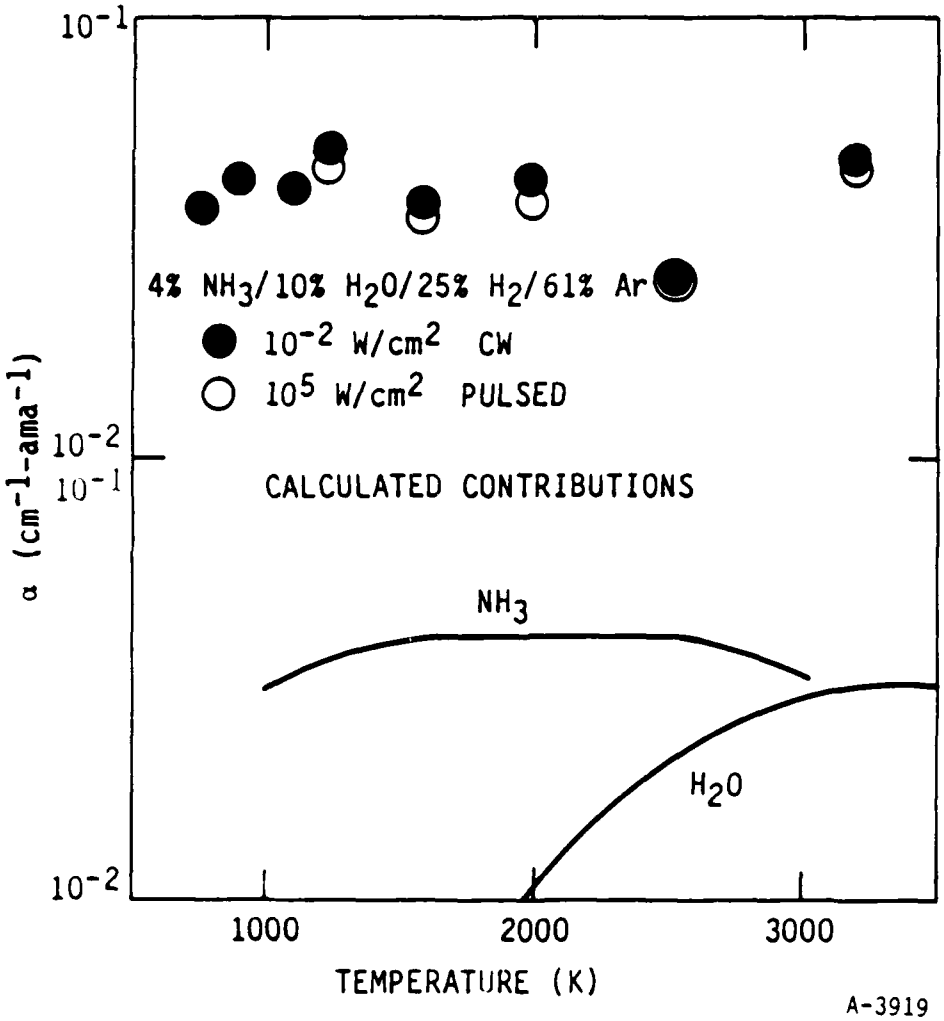

Figure 3. Absorption of $NH_3/H_2O,H_2/Ar$ mixture at 10.6 μm

spread out over 10 to 20 lines as opposed to only one line in CO_2 operation. Not all lines of the DF and HF lasers are strongly absorbed by the D_2O and H_2O and therefore the fractional absorption is significantly less than that for H_2O at 10.6 μm, and was approximately at the noise level of the detection system (2 to 5 percent). Unlike absorption at 10.6 μm, absorption at 2.7 μm for H_2O or 3.8 μm for D_2O occurs on a fundamental vibration/rotation frequency and is not expected to change significantly with temperature.

In order to perform some measurements at a shorter wavelength we investigated the absorption of the HF laser by hot, chemically generated HF. Hydrogen fluoride is highly reactive, and is not easily handled. It can be readily made by reaction of SF_6 and H_2 at elevated temperature by the global mechanism

$$SF_6 + 4H_2 \rightarrow 6\ HF + H_2S$$

This reaction is used in the pulsed HF laser to generate the excited HF, and since both components are readily storable, it represents a very reliable mixture for HF laser operation. The reaction is very fast above 1500 K and goes to completion well within the measurement time above this temperature. Two mixtures were used 0.5%SF_6/9.5%H_2/90% Ar and 1%SF_6/9%H_2/90%Ar. The results of these measurements are shown in Figure 4. Above 1500 K the absorption coefficient is constant to above 3500 K. The laser intensity was ~1.4 x 10^5 W/cm^2, and no saturation effects are observed.

2.1.3 Summary of the experimental shock tube measurements--In the overall course of this multi-year program we have measured the absorption coefficient of CO_2, H_2O, NH_3, NF_3, and SF_6 at 10.6 μm and HF at 2.7 μm. It has been shown that mixtures of $H_2O/NH_3/H_2$ can be used as a propellant system for a CW CO_2 laser heated rocket thruster and that SF_6/H_2 (HF) is an excellent propellant mixture for HF laser wavelengths. By inference, SF_6/D_2 (DF) should work equivalently with all DF laser wavelengths.

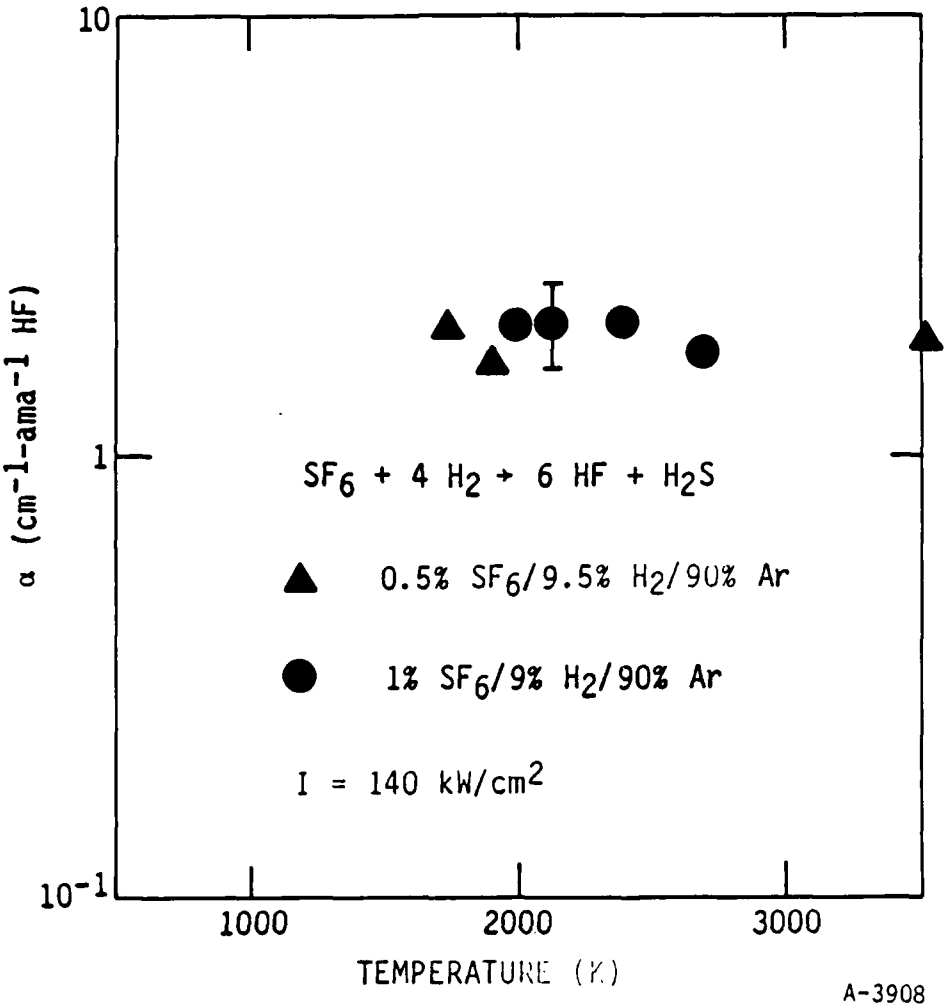

Figure 4. Absorption coefficient of HF versus temperature

2.2 PULSED THRUSTER MODELING

The main modeling activity during this period has been aimed at exploring the relationship between propulsive performance of a pulsed, laser-heated thruster, and the controllable input parameters. Examples of such parameters are the energy deposited in the propellant gas, the mass flow rate, and the degree to which the nozzle is filled.

To conduct this exploration, we used a computer model, developed over the past five years, which models the non-steady, quasi-one-dimensional flow of a laser-heated real gas in a nozzle of arbitrary shape. This program has been specially developed to model the flow in pulsed, laser-heated thrusters. It includes chemical equilibrium for the propellant gas, absorption coefficients appropriate to the laser wavelength of interest, and partial filling of the nozzle to simulate one of a train of pulses. Rather detailed descriptions of the development of this program can be found in Refs. 3 and 10.

To calculate the propulsive performance of the nozzle, one first finds the force on the nozzle as a function of time, then the time integral of the force, which is the impulse, and then the specific impulse.

The force is easily calculated, in the quasi-one-dimensional approximation, by integrating the pressure p over the cross-sectional area A(x):

$$F(x,t) = \int_0^x p(x',t)dA(x')$$

The impulse is

$$I(x) = \int_0^t F(x,t')dt'$$

For a pulsed thruster, the specific impulse is best defined as the impulse divided by the mass in the nozzle when the pulse starts, and also divided by the acceleration of gravity:

$$I_{sp}(x) = I(x)/\left(m(x)g\right)$$

These three quantities are all calculated by the computer program at each axial station x.

There are a number of parameters which can be varied in the computer model to simulate different operating conditions. One is the mass flow rate which fills the nozzle, controlled by the pressure in the gas reservoir. A second is the time interval during which this gas flows, which determines how much mass is in the nozzle when the laser fires. A third is the amount of laser energy absorbed in this gas.

One of the features of the computer model is a shut-off of the mass flow into the nozzle when the calculation starts. There is no further flow into the nozzle from the reservoir during the course of the calculation. This shut-off is caused by the high pressure generated by absorption of laser energy, which prevents the reservoir from feeding any more propellant gas through the throat into the nozzle. Therefore, only the mass of gas loaded into the nozzle when the calculation begins is available for propulsion. As pointed out above, this mass can be varied in two ways. The reservoir pressure controls the mass flow rate (and the density level), and so provides one parameter. The time during which the nozzle is allowed to fill, before turning on the laser, determines the duration of the mass flow, and thus the amount of mass in the nozzle, as well as the length of nozzle filled with this gas. This time provides the second parameter.

Intuitively, one might expect that the specific impulse (I_{sp}) produced by a laser-powered pulsed thruster would depend on the energy per unit mass deposited in the propellant gas. A large amount of energy deposited in a small amount of gas should lead to a high I_{sp}, and vice-versa. Calculations made with the computer model were used to test this idea.

References 3 and 10 report experiments performed at PSI on a laboratory scale to establish the feasibility of pulsed laser propulsion. The computer

model has been used to calculate the nozzle flows resulting from the geometrical and physical parameters used in some of those experiments.

The nozzle geometry was conical, with a 10° half angle, a 1 mm throat diameter, and a length of 10 cm. Two reservoir pressures were used, 5 and 10 atm, which correspond for this nozzle to mass flow rates of 0.27 and 0.54 g/s. Fill times used were 10 and 20 μs. These were combined so as to produce two different values of mass m in the nozzle, 5.5×10^{-6} and 1.12×10^{-5} g. These values correspond to 10 and 20 μs fills at 0.54 g/s, and the smaller value to a 20 μs fill at 0.27 g/s.

The laser used for the laboratory experiments had a nominal energy E of 9J per pulse. In fact, the output varied from 2 to 9J, and this was the range of energy used in the calculations.

These values of m and E led to a range of values of E/m from roughly 2×10^5 to 2×10^6 J/g.

Figure 5 shows the results of some of these calculations, plotted as I_{sp} versus E/m, the amount of deposited energy per unit mass. The circles are for a mass flow of 0.54 g/s, and they are fitted very well by a straight line in the log-log plot. The square point is at $\dot{m} = 0.27$ g/s and also fits rather well on the line. This plot shows that E/m is the primary parameter which determines I_{sp}. The values of I_{sp} range from 1000 to 4400s, giving encouraging evidence that pulsed laser propulsion can produce high values of specific impulse.

The equation of the line in Figure 5 is

$$I_{sp}(s) = 0.45[E/m(J/g)]^{0.644}$$

The object of pulsed laser propulsion is, of course, to produce thrust. This is accomplished, as in any fluid propulsion system, by converting the energy supplied (laser energy) into directed kinetic energy at the nozzle exit.

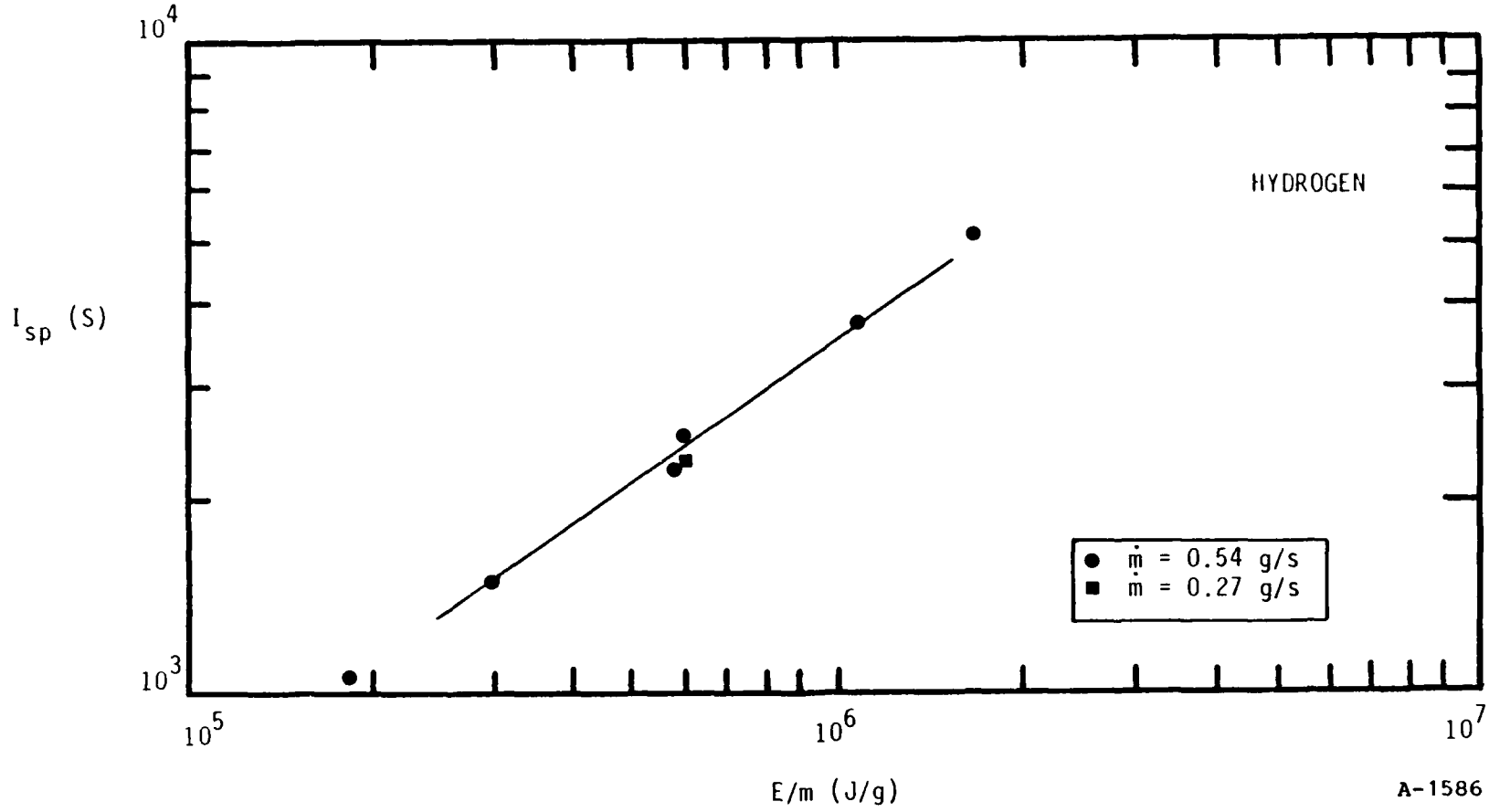

Figure 5. Calculated specific impulse for a pulsed laser-heated thruster with hydrogen propellant. Abscissa is the laser energy deposited per unit mass in the nozzle.

In laser propulsion schemes, the laser energy is first absorbed in the propellant gas, heating it to high temperatures. At this stage, the energy is invested in translation and the internal degrees of freedom, including dissociation and ionization. During the expansion of the gas through the nozzle, the energy feeds out of these degrees of freedom, into directed kinetic energy. It is clearly important to get as much energy into directed kinetic energy as possible, to maximize the thrust produced. Energy which remains in translation (temperature) or internal degrees of freedom at the nozzle exit does not contribute to thrust.

If rates of de-ionization and recombination are not fast enough, compared to the residence time of the gas in the nozzle, energy can remain in internal degrees of freedom. The best one can achieve here is for the gas to stay in local chemical equilibrium as it expands, and this is the assumption that has been made in the calculations reported here. The adverse effect of non-equilibrium composition should be looked at, but it requires a knowledge of reaction rates which is not very well-established for hydrogen, for example.

Even if equilibrium is assumed, the rate of expansion in the nozzle determines the conversion of internal and translational energy into directed energy. This, in turn, depends on the nozzle geometry, the flow parameters, and the amount of laser energy absorbed.

In the calculations made here, the division of energy into its various components was monitored as the calculation proceeded. Four quantities were plotted.

(1) The fluence of total energy at each nozzle station X at each time t.

$$\mathrm{NRGFLU} = \int_0^t \rho u A\left(h + u^2/2\right) dt$$

Here ρ is gas density, u axial gas velocity, A nozzle cross-section area, and h gas enthalpy.

(2) The fluence of kinetic energy

$$KEFLU = \int_0^t \rho u A\left(u^2/2\right)dt$$

(3) The fluence of energy in dissociation

$$CHEMNRG_D = \int_0^t \rho u A(e_{diss})dt$$

where e_{diss} is the energy per unit mass of gas tied up in dissociation.

(4) The fluence of energy in ionization

$$CHEMNRG_I = \int_0^t \rho u A(e_{ion})dt$$

where e_{ion} is the energy per unit mass of gas tied up in ionization.

As an example of the partition of energy, we present plots of the above four fluences in Figures 6, 7, and 8. In each plot, the abscissa is the axial distance X, in cm. The various curves are for different times, which are given in each plot in the upper right corner as TMD, in μs. A point on a curve represents the amount of energy which has flowed past the axial station X up to the time TMD.

For the run shown in these figures, 3.25J of laser energy was initially put into the gas contained in 1.46 cm of the nozzle. Then the calculation was started. The mass flow rate of hydrogen to fill the nozzle was 0.54 g/s (p_{res} = 10 atm), and the nozzle was filled for 20 μs, so the fresh gas extended to 5.6 cm in the nozzle.

Figure 6 shows the total energy fluence, NRGFLU in erg. The energy is initially contained near X = 1.46, but spreads downstream as time progresses. By 15 μs, nearly the whole 3.25J has passed the 10 cm station.

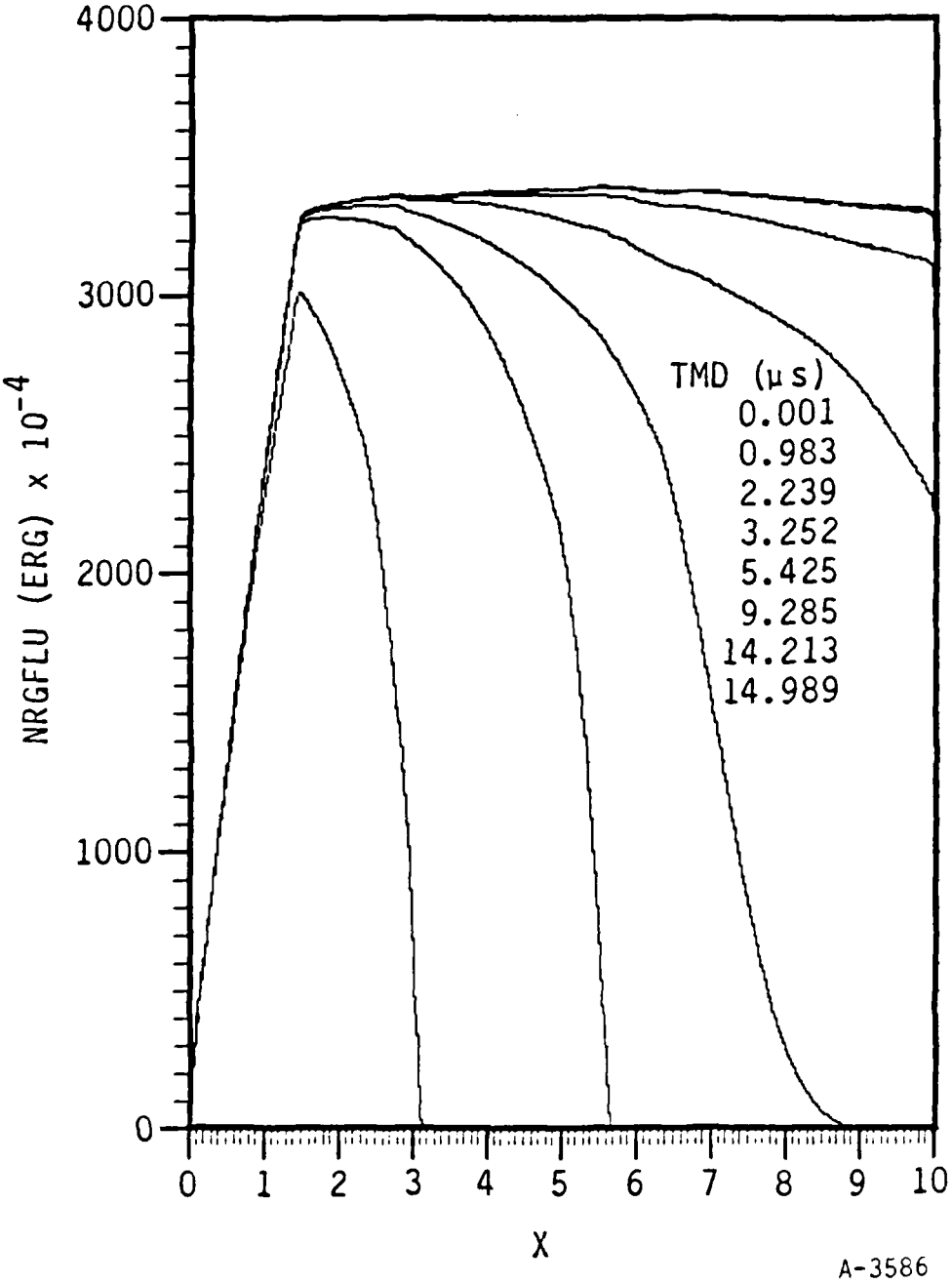

Figure 6. Total energy fluence profiles at various times. Hydrogen propellant. 0.54 g/s (10 atm) fill rate. 3.25J of laser energy deposited in 1.46 cm of nozzle gas. Nozzle filled for 20 μs (up to 5.6 cm).

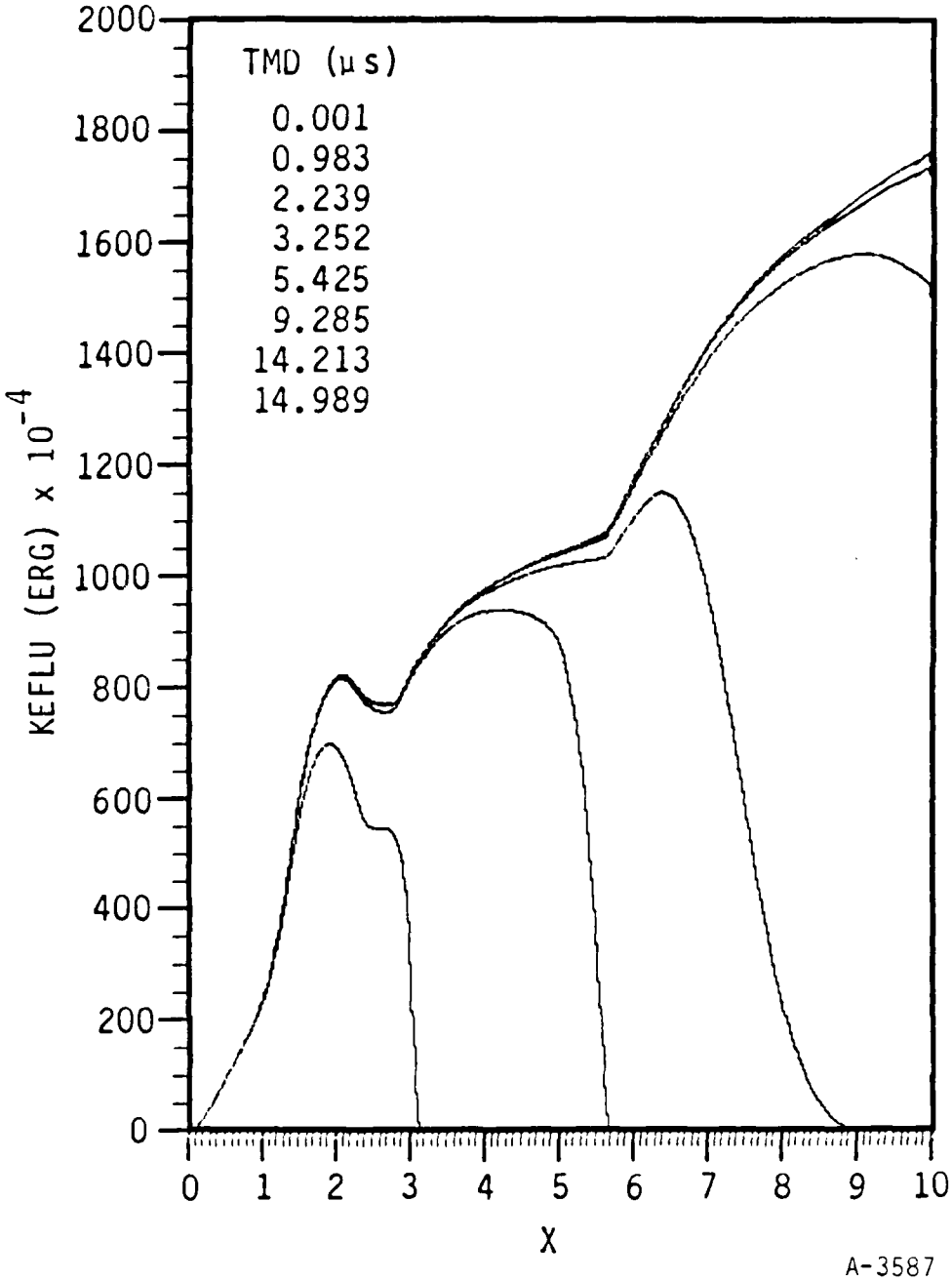

Figure 7. Kinetic energy fluence profiles at various times. Conditions as given in Figure 4.

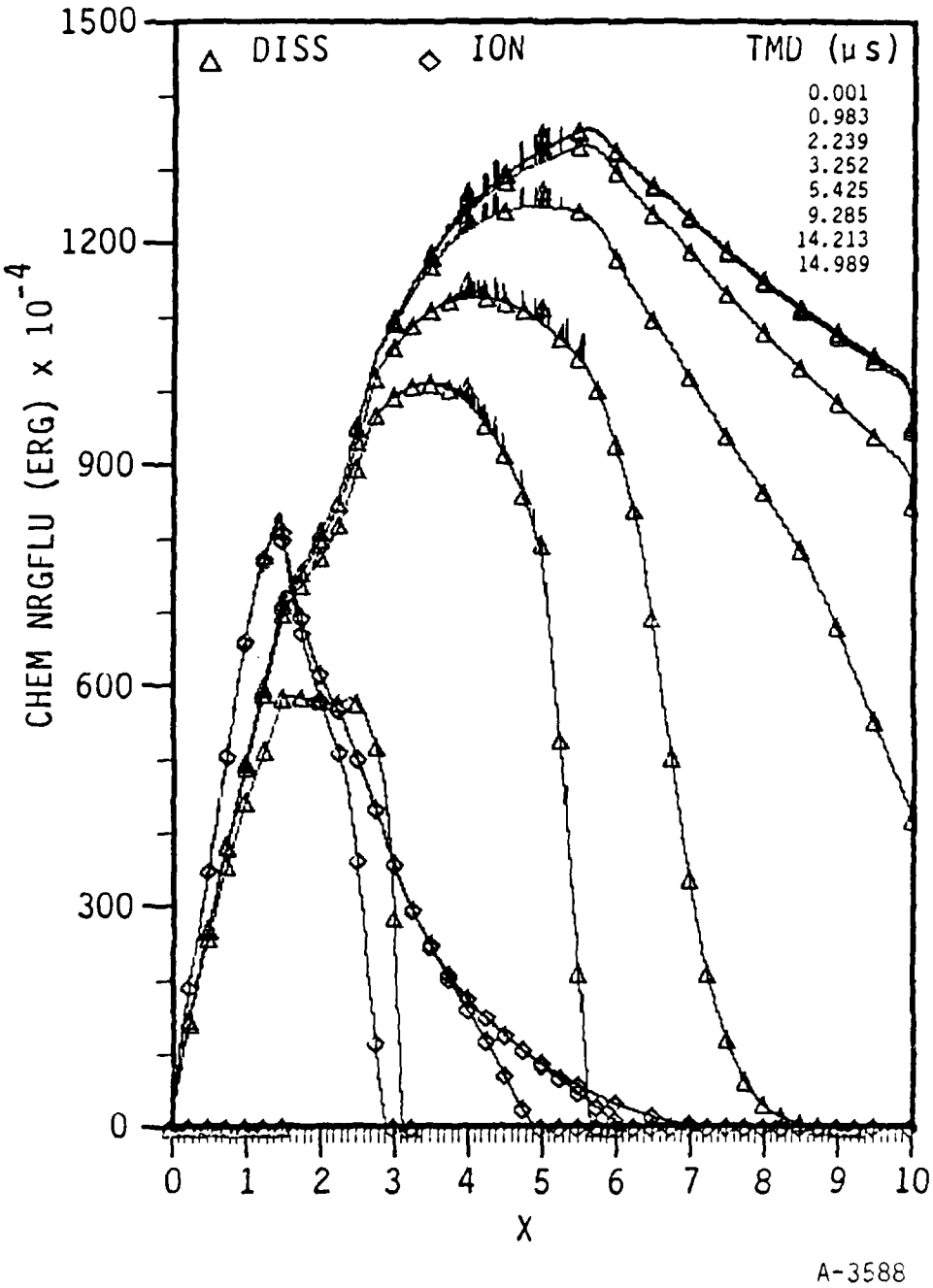

Figure 8. Dissociation and ionization energy fluence profiles at various times. Conditions as given in Figure 6.

Figure 7 shows the kinetic energy fluence, KEFLU. Only about 1/5 of the energy fluence is kinetic at short times, but more and more energy appears in this form as time progresses. By 15 μs, 1.75J has passed 10 cm as kinetic energy, which is about 54 percent of the laser energy.

Figure 8 shows the ionization energy fluence (diamonds) and the dissociation energy fluence (triangles). At early times, when all the laser energy has been put into a small amount of gas, there is a lot of ionization energy which has passed 1.5 cm (0.8J), but almost none has passed 3 cm. Less dissociation energy has passed 1.5 cm (0.6J) because the gas is at such a high temperature that ionization dominates. At later times, as the hot gas progresses down the nozzle and cools, the ionization energy fluence passing larger X stations vanishes. Only dissociation energy is carried to large X. At 15 μs, its fluence peaks at 5.5 cm (1.35J), and is down to 1J at 10 cm because of further cooling.

Thus at 15 μs and 10 cm, 1.75J has passed as kinetic energy, 1J as dissociation energy, and the remaining 0.5J (out of 3.25J) has passed as translational energy (temperature). As mentioned above, this represents a 54 percent conversion of laser energy to kinetic energy.

Other runs show similar trends. There will be an effect of nozzle geometry on this energy conversion, but we have not explored different geometries.

3. WRITTEN PUBLICATIONS IN TECHNICAL JOURNALS

1. Kemp, N.H. and Rosen, D.I., "Energy Deposition of Pulsed 1.0 Micron Laser Radiation in Gases," Paper AIAA-85-155, AIAA 18th Fluid Dynamics and Plasmadynamics and Lasers Conference, July 16-18, 1985.

2. Krech, R.H., Cowles, L.M., Caledonia, G.E., and Rosen, D.I., "Linear and Non-linear Absorption of Hot SF_6 and NH_3 at 10.6 μm," Proceedings of the 15th International Symposium on Shock Tubes and Waves, Berkeley, CA.

3. Krech, R.H., Cowles, L.M., Caledonia, G.E., and Rosen, D.I., "The High Temperature Absorption of CO_2 Laser Radiation by SF_6, NF_3 and NH_3," accepted for publication in the Journal of Quantitative Spectroscopy and Radiative Transfer.

4. Weyl, G. and Rosen, D., "Laser-induced Breakdown in Nitrogen and the Rare Gases at 0.53 and 0.35 μm," submitted for publication in Journal of Physics D, September 1986.

5. Krech, R.H., Campbell, J.P., Caledonia, G.E., and Rosen, D.I., "Linear and Nonlinear Absorption of Hot H_2O and H_2O/NH_3 Mixtures at 10.6 μm," manuscript in preparation as note for AIAA Journal.

4. LIST OF PROFESSIONAL PERSONNEL ASSOCIATED WITH RESEARCH EFFORT

Dr. David I. Rosen - Program Manager and Co-investigator for pulsed thruster studies.

Dr. Nelson H. Kemp - Principal Investigator for pulsed thruster performance studies.

Mr. Robert H. Krech - Principal Scientist reponsible for carrying out shock tube absorption experiments.

Mr. George E. Caledonia - internal technical advisor for shock tube absorption studies.

5. INTERACTIONS (COUPLING ACTIVITIES)

- Oral presentation "Energy Deposition of Pulsed 1.0 Micron Laser Radiation in Gases' by N.H. Kemp at AIAA 18th Fluid Dynamics and Plasmadynamics and Lasers Conference, Cincinatti, OH (July 1985).

- Oral presentation "Absorption of CO_2 Laser Radiation in Hot SF_6, NF_3, and NH_3" by R.H. Krech at 15th International Symposium on Shock Waves and Shock Tubes, Berkeley, CA.

- Participation by D. Rosen and G. Caledonia in Solar Plasma Propulsion Workshop, Dayton, OH (January 1986).

- Two oral presentations at 1986 AFOSR/AFRPL Rocket Propulsion Research Meeting, Lancaster, CA (September 1986).

  - "Linear and Saturated Absorption of Laser Radiation in Heated Gases," R.H. Krech, L. Cowles, G.E. Caledonia, D. Rosen, and J. Campbell - presented by G. Caledonia.

  - "Performance Modeling of a Pulsed Laser Heated Thruster," N.H. Kemp and D.I. Rosen - presented by N. Kemp.

REFERENCES

1. Rosen, D., Weyl, G., Kemp, N., Ham, D., Cowles, L., and Schertzer, S., Experimental and Theoretical Studies of Laser Propulsion Phenomenology, Interim Scientific Report, No. TR-371, Physical Sciences Inc., Andover, MA, March 1984.

2. Rosen, D., Caledonia, G., Kemp, N., Krech, R., and Cowles, L., Experimental and Theoretical Studies of Laser Propulsion Phenomenology, PSI TR-505, Physical Sciences Inc., Andover, MA, March 1985.

3. Rosen, D., et al., Pulsed Laser Propulsion Studies, Vol. I: Thruster Physics and Performance, Final Technical Report No. TR-184, Physical Sciences Inc., Andover, MA, October 1982.

4. Kemp, N.H., "Computer Simulation of the Non-steady Flow of a Real Gas with Laser Energy Absorption," Paper AIAA-84-1569 AIAA 17th Fluid Dynamics, Plasma Dynamics, and Laser Conference, Snowmass, CO, June 1984.

5. Kantrowitz, A., Astronautics and Aeronautics, 10, No. 5, p. 74, May 1972.

6. Weiss, R.F., Pirri, A.N., and Kemp, N.H., Astronautics and Aeronautics, p. 50, March 2, 1979.

7. Kemp, N.H., Rosen, D.I., and Legner, H.H., "Laser Energy Absorption in Gases: Research Problems," Orbit-Raising and Maneuvering Propulsion: Research Status and Needs, AIAA Progress in Astronautics and Aeronautics, L.H. Caveny, ed., Vol. 89, p. 73, AIAA, NY.

8. Rosen, D.I., Pirri, A.N., Weiss, R.F., and Kemp, N.H., "Repetitively-Pulsed Laser Propulsion: Needed Research," p. 95, Ref. 7.

9. Kemp, N.H. and Legner, H.H., "Steady (Continuous Wave) Laser Propulsion: Research Areas," p. 109, Ref. 7.

10. Rosen, D.I., et al., Studies of a Repetitively-Pulsed Laser Powered Thruster, Final Technical Report No. TR-358, Physical Sciences Inc., Andover, MA, January 1983.

APPENDIX A

LINEAR AND NONLINEAR ABSORPTION OF HOT SF_6, AND NH_3 AT 10.6 μm* (SR-225)

*To be published in Proceedings of 15th International Symposium on Shock Tubes and Shock Waves

PSI-039
SR-225

LINEAR AND NONLINEAR ABSORPTION OF HOT SF_6, AND NH_3 AT 10.6 μm

BY

R.H. Krech, L.M. Cowles, G.E. Caledonia and D.I. Rosen

A series of shock tube measurements to determine the laser absorption coefficients of hot SF_6 and NH_3 were conducted on the 10.6 μm P(20) CO_2 laser transition. Measurements were made behind both incident and reflected shocks from 500-3000K at pressures from 10 to 70 atm. Simultaneous high intensity (100 kW/cm^2) and low intensity (1 mW/cm^2) measurements were made in NH_3 to determine if saturation would occur under the temperature and pressure conditions to be encountered in a laser-heated rocket thruster. No indication of saturation was observed and the results can be described by a simple two-level model verified by room temperature saturation measurements with SF_6.

1. INTRODUCTION

The concept of using energy, beamed from a remotely stationed laser, to power a rocket thruster is attractive since it provides high specific impulse at high thrust levels.[1-4] When a high power CW laser is used to heat the propellant, the physical processes involved are simply described by a direct, high pressure gas-phase absorption of the beam in a stagnation chamber followed by a supersonic expansion of the hot gas through a nozzle. Stagnation conditions yielding a specific impulse of 1000s can be obtained if the equivalent of nine 10.6 μm photons per molecule are absorbed into a propellant mixture where hydrogen is the primary constituent.

The original CW laser propulsion concept required a laser induced breakdown in a pure hydrogen propellant followed by the formation of a stable laser supported combustion (LSC) wave. Absorption occurs via inverse electron bremsstrahlung which requires that a significant fraction of the hydrogen be ionized. In pure hydrogen ionization becomes significant above 10,000K, with a stable LSC wave forming at approximately 20,000K. Such high temperature would create a severe thermal environment in the stagnation chamber of the thruster and thus motivated a study of seeding the propellant with alkali metals to produce electrons at lower temperatures. The addition of cesium, which thermally ionizes above 3000K, would allow the formation of an LSC wave at temperatures below 10,000K, and thus provide a less severe environment, however, it is not yet clear that the LSC wave would stabilize at such low temperatures.

Alternatively, molecules having optical transitions at the laser wavelength can absorb energy, and by collisional energy transfer, heat the hydrogen propellant.[5] The primary advantage is that formation of a stable LSC wave is not required to process the hydrogen since the heating is continuous from the inital injection temperature to the final stagnation temperature. Furthermore, if molecular absorption can heat the gas to 3000-5000K, then specific impulses of 1000-2000s can be obtained with ionization (and cesium seeding).

The high resolution absorption properties of most potential absorbers are not well known at temperatures over 1000K, especially at the pressure conditions that are required for thruster operation (10 to 100 atm). Important absorption paths due to hot bands cannot be adequately probed at low temperatures, and

indeed most molecules dissociate in the temperature range of interest. Finally, it is not known to what extent saturation will limit absorption at high irradiance levels, i.e., 1-1000 kW/cm^2. The propellant heating rate in a CW laser heated thruster is determined by the absorbed incident laser intensity. Above the optical saturation intensity, further energy cannot be absorbed due to depletion of the population of the absorbing states. Since saturation is primarily a function of the collisional relaxation time of the absorbing species, the saturation intensity of the propellant mixture will vary with composition, temperature and pressure. The lack of adequate data in the temperature and pressure range of interest for thruster operation has motivated a series of laser absorption studies in shock heated gas mixtures Potential molecular seed species studied thus far included H_2O, CO_2, NH_3, SF_6 and NF_3.

The high temperature absorption properties of $H_2O/H_2/Ar$ mixtures at 10.6 μm have been reported previously.[6,7] These measurements indicated that an additional absorber species would be required below 2000K for thruster operation. This paper presents the results of recent measurements of the 10.6 μm P(20) CO_2 laser absorption coefficients of SF_6 and NH_3 from room temperature to approximately 3000K. In the NH_3 experiments, simultaneous measurements were conducted at low intensity (1 mW/cm^2), and high intensity (100 KW/cm^2) to directly ascertain whether saturation might occur at high incident intensity.

2. EXPERIMENTAL

The laser absorption coefficient measurements were performed behind both incident and reflected shocks in a 1.5 inch diameter double diaphragm shock tube with a 5 foot long driver and a 12 foot long driven section. Optical measurements were made through anti-reflection coated zinc sulfide windows located one inch from the end wall in a 5 foot long test section with a 1.31 inch square cross section. Shock pressure was measured by four piezoelectric pressure transducers located at one foot intervals along the test section. Shock velocity is measured from the time of arrival of the incident shock wave at successive stations. The last transducer is located at the optical port to allow a direct correlation of the absorption with total pressure.

The optical configuration used for the low intensity CW laser absorption coefficient measurements is shown in Figure 1. A line-tuned, waveguide CO_2 laser (California Laser Corp. Model 81-5500-TG-T) is the CW radiation source. The main beam traverses the shock tube and a reference beam is split off near the laser source to provide a continuous measurement of the laser output. Both beams are detected by HgCdTe detectors which have linear responses at the operating intensities. The detector outputs are amplified, and digitized by a Camac data acquisition system at a 1 MHz rate, and stored in a computer for analysis. A monochromator (PTI Optics Mini-Chrom-1) is mounted in front of the transmission detector to eliminate any background emission that may exist outside the narrow bandwidth of the laser line being studied. Transmitted light is collected and focused on the entrance slit of the monochromator with an AR coated Ge lens. CaF_2 attenuators are mounted in beam path to limit the intensity through the shock tube and on the detectors. Typically the incident intensity was restricted to 1 mW/cm^2 and the power incident on the detector below 500 μW.

The high intensity measurements required that a pulsed CO_2 be coupled into the optical path, together with a dual beam pulsed detection system. This configuration is shown in Figure 2.

The pulsed laser (Lumonics TEA K-203) was operated line-tuned on a single mode without N_2 to obtain a triangular pulse with a width of 0.2 μs. The pulsed

beam was directed by two gold mirrors to a germanium beam splitter situated ten degrees off axis. The reflected beam was directed to a Laser Precision RJP-735 pyroelectric probe to monitor the laser energy. The transmitted beam is next directed to a NaCl beam splitter at Brewster's angle where it is mixed with the CW beam. From this point onward the beams are coincident. A third turning mirror directs the beams to the shock tube, where a 30 cm focal length BaF2 lens located 15 cm from the center of the test section is used to concentrate the beams. The incident intensity can be adjusted by CaF_2 attenuators and/or by repositioning the lens. After passage through the test section the beams are separated by a second NaCl beam splitter at Brewster's angle. The pulsed beam is transmitted and detected by a second RJP-735 probe. The pulsed detectors are connected to a Laser Precision 7200 Ratiometer where the energy incident on both detectors is recorded on a digital readout.

The wavelength of both the CW and pulsed CO_2 laser was determined by an Optical Engineering Spectrum Analyzer before each test.

Gas mixtures were prepared in a 31.4 liter stainless steel mixing tank. The partial pressure was monitored by a Validyne DP-15 pressure gauge. The gases were taken directly from the cylinders without further purification. Stated purities were: Ar-99.999%; SF_6-99.8%; NH_3-99.998%; H_2-99.999%.

The temperatures behind the incident and reflected shocks were calculated from the measured incident shock velocity for both frozen and equilibrium cases using the standard Rankine-Hugoniot real gas relationships. When different post shock conditions were obtained from the calculations: i.e., where dissociation of the absorber occurs, a kinetics code was used to determine the gas temperature and density history after shock passage.

The absorption coefficient α is determined by measured optical transmission, I/I_o, total pressure P, temperature T, path length ℓ, the initial mole fraction of absorber Xi, by the following equation:

$$\alpha_{(cm^{-1}\text{-}ama^{-1})} = \frac{\ell n\ (I_o/I)}{X_i\ P_{(atm)}\ \ell_{(cm)}\ \left(\frac{273}{T(K)}\right)}$$

3. RESULTS AND DISCUSSIONS

The first set of measurements were conducted with 0.0006 SF_6/0.9994 Ar mixtures on the 10.6 μm P(20) CO_2 laser transition from 500 to 2500K at pressures from 10 to 70 atm. SF_6 was chosen since it is one of the most efficient absorbers of CO_2 laser radiation, and is a known saturable absorber.

A typical absorption signal obtained during the SF_6/Ar tests is shown in Figure 3. The peak of the band is located at 948 cm^{-1} at room temperature and due to the anharmonicity in SF_6 shifts to lower frequencies as the temperature is increased.[8] Therefore the absorption coefficient decreases with increasing temperature, and the room temperature absorption is higher than that of the shock heated gas even though the density is higher after shock passage. The results of our measurements are shown plotted in Figure 4, together with fits obtained from the experimental measurements of Nowak and Lyman.[8] The measured absorption coefficients are in reasonable accord with the previous values, although a slight divergence is noted at the lower temperatures.

At the pressures of interest to laser propulsion, the absorption is due to many overlapped transitions in the SF_6 and the entire vibrational manifold is involved in the absorption process. Therefore a simple two level saturation model is sufficient to describe the absorption:

$$x + h\nu\ (10.6\ \mu m) \rightarrow x^*$$

$$x^* + M \rightarrow X + M\ .$$

It can be shown that the CO_2 laser absorption coefficient α at any intensity I is related to the low intensity absorption coefficient α_o, as a function of the quench rate, kq and total quencher density M, by

$$\alpha = \alpha_o \frac{kq\ M}{(kq\ M + 2\ \alpha_o\ (ama^{-1}cm^{-1})\ I\ (W/cm^2))}\ .$$

To verify the model, a series of room temperature saturation measurements were conducted in SF_6/Ar mixtures at atmospheric pressure. The results are shown in Figure 5. On the P(20) laser transition, the low intensity room temperature SF_6 absorption coefficient is ~300 cm^{-1}-ama^{-1}. At atmospheric density ($M = 2.6 \times 10^{19}\ cm^{-3}$), and a quench rate of $3 \times 10^{-13}\ cm^3/s$, the predicted absorption coefficient is reduced by half at an intensity of 14 KW/cm^2. This is in reasonable accord with the data.

The third series of measurements were conducted in 0.094 NH_3/0.906 Ar and 0.05 NH_3/0.45 H_2/0.50 Ar mixtures on the P(20) CO_2 laser transition from 900 to 2900K at pressures from 10 to 40 atm. A typical absorption signal in the NH_3/Ar series is shown in Figure 6 for a reflected shock temperature of 2315K. A fairly rapid decay of the signal is observed after the reflected shock. Simultaneous measurements were made of the low and high intensity absorption coefficients behind the reflected shock, and the spike in the trace is a result of the pulsed laser. No difference in absorption was noted between absorption coefficients obtained from the pulsed measurements at intensities slightly in excess of 100 KW/cm^2 and those obtained with 1 mW/cm^2, indicating that ammonia is not saturating under the conditions behind the reflected shock.

The dissociation of the absorber species below the stagnation temperature is not desirable. In the absence of significant concentrations of H_2, the disappearance of NH_3 is rapid. Equilibrium calculations predict that even with H_2 added to the mixture to shift the equilibrium towards NH_3, the concentration of NH_3 behind the reflected shock above 1500K will be too low to give significant absorption if equilibrium is attained. The kinetics of ammonia decomposition are reasonably well known and indicates that below 2500K little decomposition occurs if a substantial fraction of the propellant is H_2. The $H_2 + NH_2 \rightarrow H + NH_3$ reaction plays a major role in regenerating NH_3 and slowing the overall decay rate. Figure 7 shows that the NH_3 absorption signal does not decay in the several hundred μs of available test time at 2290K with 45% H_2 in gas mixture. The results of our measurements are shown in Figure 8. Under all test conditions the absorption coefficients obtained from the pulsed laser matched those obtained at low intensity with CW laser.

From the two level saturation model presented above, the intensity required to obtain significant saturation is shown to be inversely proportional to the low intensity absorption coefficient. As the absorption coefficient of NH_3 is between 1 and 2 cm^{-1}-ama^{-1} above 1000K, saturation should not occur at the intensities encountered in our pulsed measurements, and indeed none was observed.

4. CONCLUSIONS

The absorption coefficients for potential laser heated thruster propellant additives are shown in Figure 9. At temperature below 1500K, SF_6 is by far the best absorber on a weight basis, but since SF_6 will react with H_2 it is not the most desirable low temperature absorber. NH_3 is a strong absorber which does not rapidly decompose in the presence of H_2 from room temperature to 3000K. Above 3000K, H_2O is the best absorber. A significant absorption advantage is gained by chemical nonequilibrium during the short flow times (hundreds of μs) involved in these experiments and appropriate to a CW laser heated thruster. This study suggests that a propellant mixture containing NH_3, H_2O, and H_2 is suitable for a high performance laser heated rocket thruster powered by a CW CO_2 laser.

ACKNOWLEDGEMENTS

This work was sponsored by the Air Force Office of Scientific Research under Contract F49620-83-C-0039 monitored by Dr. Len Caveny. The authors wish to thank Dr. David O. Ham of Physical Sciences Inc. for his help on the saturation studies.

REFERENCES

1. Caledonia, G.E., Wu, P.K. and Pirri, A.N., "Radiant Energy Absorption Studies for Laser Propulsion," Physical Sciences Inc., PSI TR-20 (NASA CR-134809), 1975.

2. Kemp, N.H., Root, R.G., Wu, P.K., Caledonia, G.E. and Pirri, A.N., "Laser-Heated Rocket Studies," Physical Sciences Inc., PSI TR-53, (NASA DR-1315127), 1976.

3. Fowler, M.C., Newman, L.A. and Smith, D.C., "Beamed Energy Coupling Studies," Final Technical Report for Contract No. F04611-77-C-0039, AFRPL-TR-79-51, September 1979.

4. Nebolsine, P.E., Pirri, A.N., Goela, J.S., Simons, G.A. and Rosen, D.I., "Pulsed Laser Propulsion," Paper VI-2, AIAA Conference on Fluid Synamics of High Power Lasers, Cambridge, MA 1978 (also PSI TR-142).

5. Caledonia, G.E., "Conversion of Laser Energy to Gas Kinetic Energy," J. of Energy, 1, 1977, p.121-124.

6. Krech, R.H., Pugh, E., "Determination of Absorption Coefficients in Shock Heated Propellant Mixtures for Laser-Heated Rocket Thrusters," 13th Int. Symp. on Shock Tubes & Waves, Niagara, NY, 1981, p.462-469.

7. Pugh, E. and Krech, R.H., "Absorptivity of Water Vapor for 10.6 μm Radiation, AIAA J., 20, 1982.

8. Nowak, A.V. and Lyman, J. "The Temperature-Dependent Absorption Spectrum of the ν_3 Band of SF_6 at 10.6 μm," J. Quant. Spectrosc. Radiat. Transf. 15, (1975), p.945.

9. Baulch, D.L., Buxbury, J., Grant, S.J. and Montague, D.C., "Evaluated Kinetic Data for High Temperature Reactions," Vol. 2, Buttersworth, London-Boston, 1976.

Figure Captions

Figure 1. Optical Setup for Low Intensity Absorptions Measurements.

Figure 2. Optical Setup for Simultaneous Low and High Intensity Absorption Measurements.

Figure 3. Typical SF_6 Absorption Trace.

Figure 4. SF_6 CO_2 Laser Absorption Versus Temperature.

Figure 5. SF_6 Laser Absorption Versus Intensity.

Figure 6. Absorption Signal From NH_3/Ar Mixture Without H_2.

Figure 7. Absorptions Signal From NH_3/H_2/Ar Mixture.

Figure 8. NH_3 Absorption Versus Temperature.

Figure 9. Absorption Coefficients Versus Temperature of Potential Seed Absorbers.

Table 1. Ammonia Decomposition Kinetics

	RATE CONSTANTS (cm^3/s, cm^6/s)
1. $NH_3 + M \quad NH_2 + H + M$	$1.5 \times 10^{-8}\ e^{-42400/T}$
2. $H + NH_3 \quad NH_2 + H_2$	$4.6 \times 10^{-11}\ e^{-8700/T}$
3. $NH_2 + H \quad NH + H_2$	$1.7 \times 10^{-13}\ T^{.67}\ e^{-2150/T}$
4. $NH_2 + NH_2 \quad NH_3 + NH$	$9.6 \times 10^{-11}\ e^{-1800/T}$
5. $NH + N \quad N_2 + H_2$	1.7×10^{-11}
6. $NH + H \quad N + H_2$	$1.7 \times 10^{-12}\ T^{.68}\ e^{-960/T}$
7. $N + N + M \quad N_2 + M$	$3 \times 10^{-32}\ T^{-0.5}$
8. $H + H + M \quad H_2 + M$	$2 \times 10^{-30}\ T^{-1}$

- REACTION 2 DETERMINES OBSERVED DECAY TIMES
- DECOMPOSITION SLOWED BY ADDITION OF H_2

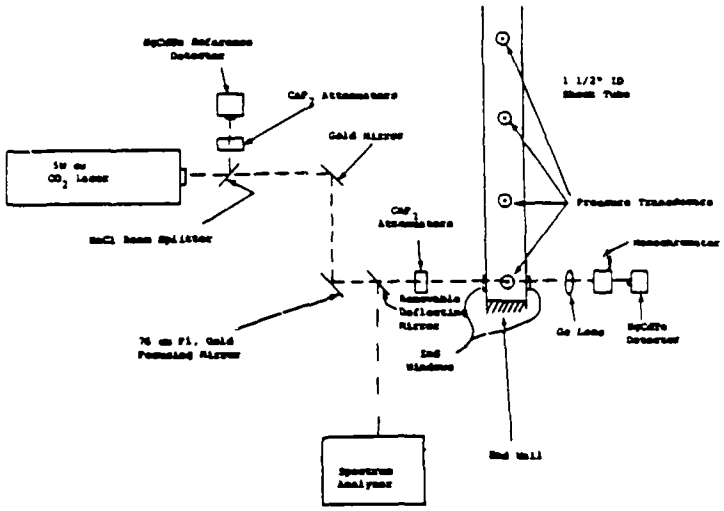

Figure 1. Optical Setup for Low Intensity Absorptions Measurements.

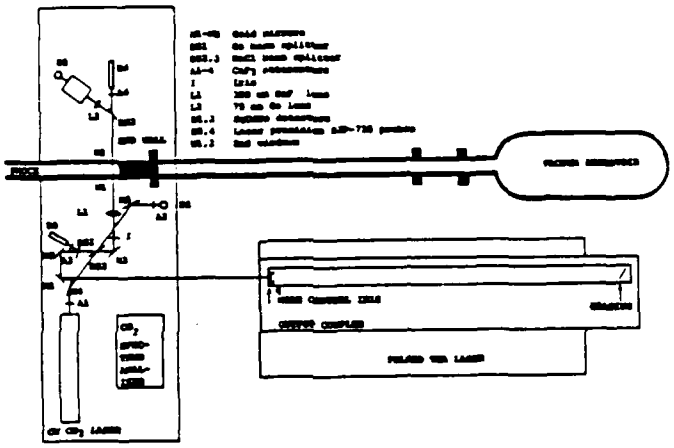

Figure 2. Optical Setup for Simultaneous Low and High Intensity Absorption Measurements.

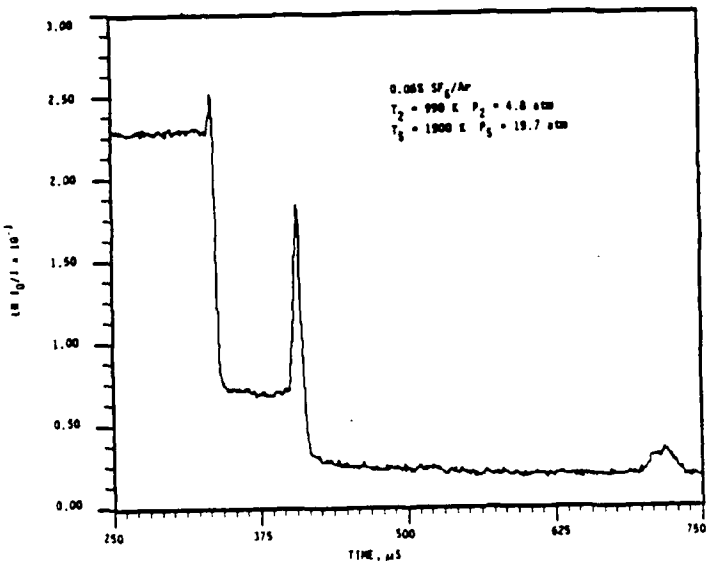

Figure 3. Typical SF_6 Absorption Trace.

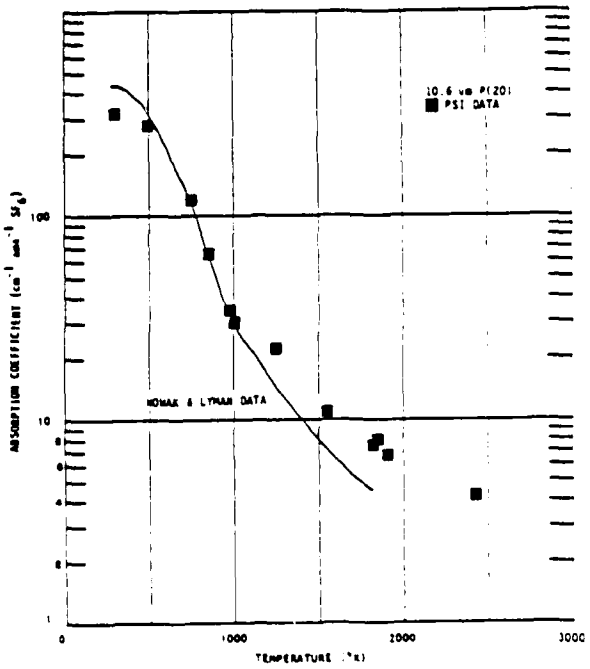

Figure 4. SF_6 CO_2 Laser Absorption Versus Temperature.

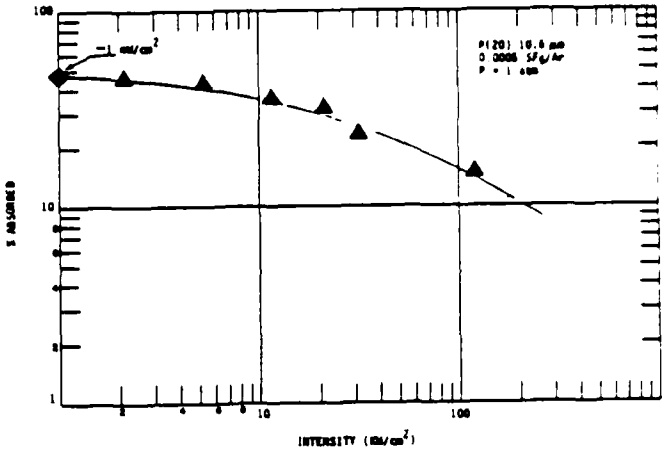

Figure 5. SF_6 Laser Absorption Versus Intensity.

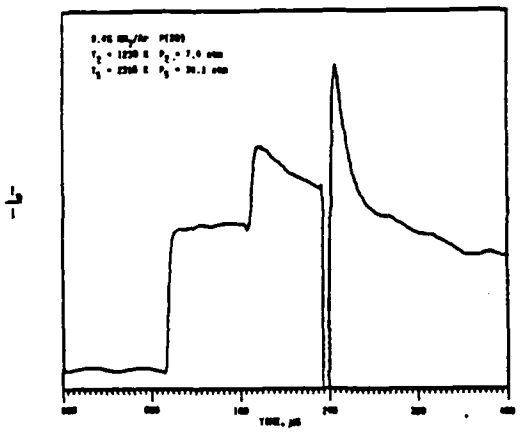

Figure 6. Absorption Signal From NH_3/Ar Mixture Without H_2.

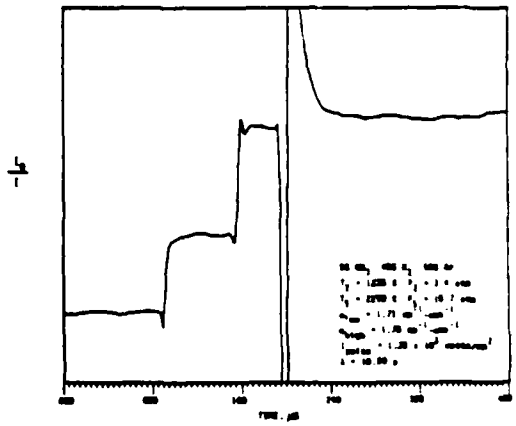

Figure 7. Absorptions Signal From NH_3/H_2/Ar Mixture.

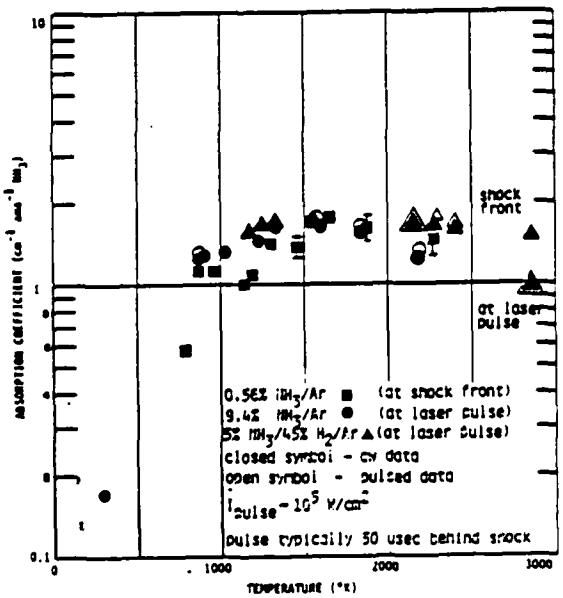

Figure 8. NH_3 Absorption Versus Temperature.

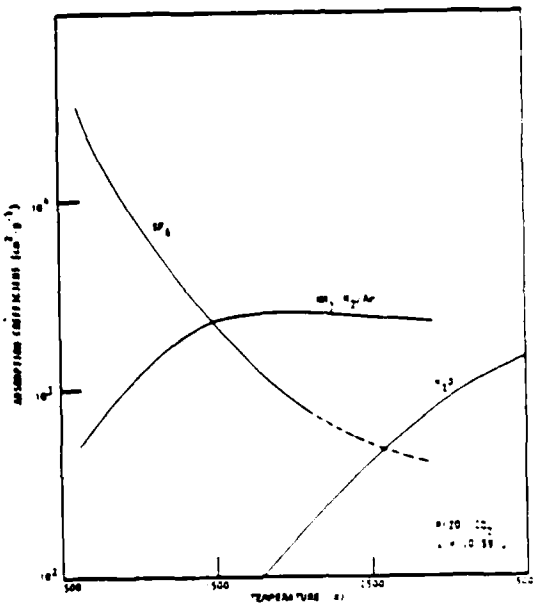

Figure 9. Absorption Coefficients Versus Temperature of Potential Seed Absorbers.

APPENDIX B

THE HIGH TEMPERATURE ABSORPTION OF CO_2 LASER RADIATION BY SF_6, NF_3, AND NH_3* (SR-250)

*Accepted for publication in JQSRT

PSI-034/
SR-250

THE HIGH TEMPERATURE ABSORPTION OF CO_2 LASER RADIATION BY SF_6, NF_3, AND NH_3

R.H. Krech, L.M. Cowles, G.E. Caledonia, and D.I. Rosen

Physical Sciences Inc.
Andover, MA 01810

Abstract

The absorption coefficients of SF_6, NF_3, and NH_3 at CO_2 laser wavelengths have been evaluated at elevated temperatures in a shock tube study. Measurements were performed in the pressure range of P = 10 to 70 atm for temperatures between 500 and 2900 K. The effects of finite rate chemical decomposition on the absorption observations are discussed.

1. INTRODUCTION

The potential use of lasers as remote sources of power for rocket propulsion has been under investigation for a number of years.[1-5] Laser propulsion specifically refers to the beaming of energy from a remote high power laser to a rocket engine. The beam power is absorbed by a working fluid in the plenum region of the engine and is converted into kinetic energy through a nozzle expansion to produce thrust. This approach combines the high specific impulse (greater than 1000s) of ion propulsion with the high thrust to mass ratio of chemical propulsion, a combination not achievable by any other practical propulsion system. This unique combination of advantages is made possible both by the high temperatures which can be reached and by the reduced weight of the propulsion system. The ultimate temperature is not limited by a chemical flame temperature but only by the ability to focus, absorb, and contain the laser energy. The weight reduction is a result of the remote power source, whose mass does not have to be transported with the rocket.

One propulsion concept which is under consideration for use with CW infrared lasers involves utilizing a propellant mixture composed of molecular hydrogen seeded with trace amounts of molecular absorbers and alkalis. The object is to provide for sufficient absorption of the laser energy in seed molecule vibration-rotation absorption bands to allow heating of the working fluid from room temperature to ~3500 K. The alkalis will be ionized at this latter temperature providing a source of electrons so that further absorption by inverse electron neutral/ion bremsstrahlung will allow gas processing to even higher temperatures.

Depending upon the gas conditions and laser intensity, the absorption process can lead to highly non-equilibrium vibration and chemical

distributions. A kinetic example of CW CO laser absorption by a diatomic molecule has previously been provided.[6] Unfortunately no stable diatomic molecule has been identified for absorption of 10.6 μm CO_2 laser radiation. In this instance, one is forced to rely on triatomic or larger molecules which typically are not chemically stable at temperatures higher than 2500 K. Furthermore, with a few notable exceptions, the high resolution absorption properties of larger molecules have not been measured at temperatures above 1000 K.

For the laser propulsion application, these fundamental measurements are required for pressures between 10 to 100 atm. In general, the overlapping line approximation is valid at such pressures (i.e., the line widths of adjacent transitions are larger than the spacing between them[6]), and thus continuum band models may be developed. Nevertheless absorption data is required for validation purposes, since absorption in the wings of bands or in regions dominated by hot bands may not be predicted correctly by such models.

A shock tube study of the absorption of water vapor at 10.6 μm has previously been presented.[7] That work is extended in the present paper to include measurements of 10.6 μm radiation absorption by SF_6, NF_3, and NH_3 over the temperature range of 500 to 2900 K and pressure range of 10 to 70 atm. Preliminary results for SF_6 and NH_3, along with measurements of absorption saturation, have been presented elsewhere.[8]

2. EXPERIMENTAL DESCRIPTION

The test gases were heated through use of a 1.5 in. inner diameter stainless steel shock tube having a 5-ft long driver and 12-ft driven section. The shock waves are initiated using the double diaphragm technique, which assures shock reproducibility and minimizes uncertainties due to diaphragm thickness

or scoring. The main driver section and the intermediate chamber are simultaneously filled to 100 - 200 percent and 50 - 100 percent of the single-diaphragm bursting pressure, respectively; the diaphragm rupture is then initiated by rapidly evacuating the intermediate chamber. The diaphragms, typically 0.2 to 0.5 mm thick aluminum, are prescored in a hydraulic press to ensure rapid and uniform opening times. Steady shock test times of several hundred microseconds were standardly obtained.

The laser absorption measurements are performed through anti-reflection coated zinc sulfide windows mounted 1 in. from the end wall in a 5 ft long by 1.31 in. square test section coupled to the driven section by a 3 in. long constant area transition region. Shock pressures are measured by four piezoelectric transducers located at 1-ft intervals along the test section. Shock velocities are determined from arrival times of the shock wave at successive transducers. The last transducer is located at the optical port for direct measurement of the total pressure at the position of the transmission measurement. Absorption measurements were made behind both incident and reflected shocks to provide complete coverage of the temperature and pressure range of interest. Both hydrogen and helium driver gases have been used in order to vary the shocked gas conditions.

Gas mixtures are prepared in a stainless steel mixing tank by filling with absorber gas to the desired partial pressure and then adding Ar through a spray bar to facilitate good mixing. The mixture is then allowed to sit for at least twice the predicted mixing time. Enough mix is prepared for a full series of shocks in order to maintain consistency. The gases were taken directly from the cylinders without further purification. Stated purities were: Ar - 99.999%; SF_6 99.8%, NF_3 98%; NH_3 99.8%; and H_2 - 99.999%.

The optical configuration used for these measurements is shown in Figure 1. A line tunable, waveguide CO_2 laser (California Laser Corp., Model No. 81-5500-TG-T) provides a CW source of many lines at powers of up to a few watts for each line. The main beam traverses the shock tube and a reference beam is split off near the laser source to provide continuous measurement of the laser output. The main beam and reference beam are detected by HgCdTe detectors, which have been shown to have linear responses at the operating intensities. The signal from these detectors is amplified, digitized, and stored in a computer. A monochromator (PTR optics Mini-Chrom-1 Model No. 11550) is mounted just before the main detector to eliminate any background emission that may exist outside the narrow bandwidth of the laser line being studied. Transmitted light is collected with an anti-reflection coated Ge lens and the beam was slightly defocussed to flood the entrance slit of the monochromator so as to minimize signal variations due to Schlieren effects. A set of CaF_2 attenuators are mounted in front of the entrance window of the shock tube to control the intensity on the detector and to permit studies of possible intensity variations in the absorption. Typically the incident intensity in the shock tube was restricted to 1 mW/cm^2 and the power incident on the detector remained below 500 μW.

With this configuration only relatively small deflections of the signal are observed as a shock front of pure Ar passes. No signal is observed on either detector when the NF_3, NH_3, and SF_6 mixtures are shocked with the laser blocked.

Laser output power and stability were measured by placing a power meter (Scientech Model No. 367) directly in front of the laser. Mode shape was determined by observing the beam on a phosphorescent screen. The laser was

operated throughout this series of experiments in TEM_{00} mode. For wavelength calibration, a gold mirror is used to divert the beam into a CO_2 spectrum analyzer (Optical Engineering Model 16-A), where the laser is tuned to the desired transition.

Experimental data were collected and stored in a computer-controlled CAMAC-based data acquisition system. The system is built around two LeCroy Model 8210 Waveform Digitizers. Each unit can simultaneously sample four analog signals at a 1 MHz rate and has a 10-bit, 32 K word memory which will store 8 ms of data. After each test, the data were transferred to a PRIME 400 computer for immediate preliminary analysis and storage.

The temperatures behind the incident and reflected shocks were calculated from the measured incident shock velocity for both frozen and equilibrium cases using the standard Rankine-Hugoniot real gas relationships.[9] When different post-shock conditions were obtained from the calculations, i.e., where dissociation of the absorber occurs, a kinetics code was used to determine the gas temperature and density history after shock passage (see Section 3).

The absorption coefficient α is determined from measured optical transmission I/I_o, total pressure P, temperature T, path length ℓ, and the initial mole fraction of absorber X_i, through the following relationship:

$$\alpha_{(cm^{-1}\text{-}ama^{-1})} = \frac{\ell n(I_o/I)}{X_i \; P_{(atm)} \; \ell_{(cm)} \left(\frac{273}{T(K)}\right)} \quad . \tag{1}$$

Note that measurements were always performed at sufficiently high pressures so that absorption contributions from overlapping transitions eliminated any dependence of the absorption coefficient on total pressure.

Transmission measurement were performed behind both incident and reflected shocks on each run. Incident shock temperatures were typically below 1600 K and reflected shock temperatures above 1100 K. The shock pressures were sufficiently high so that vibrational equilibration of the absorber gases occurred rapidly behind the shock front. Chemical relaxation occurred more slowly as discussed in the next section.

3. RESULTS AND DISCUSSION

Absorption measurements were performed behind both incident and reflected shocks in mixtures of SF_6, NF_3, and NH_3, dilute in Ar and H_2, at several CO_2 laser wavelengths. A summary of the parameter space of the measurements is provided in Table 1.

3.1 SF_6

SF_6 is of particular interest because it is a very efficient gaseous absorber of CO_2 laser radiation at room temperature. Furthermore, even though SF_6 would be nearly completely dissociated under equilibrium conditions at temperatures in excess of 500 K, its decomposition kinetics are sufficiently slow so that the characteristic SF_6 dissociation time will exceed 100 μs for temperatures below 1900 K at 30 atm.[10,11] Thus, SF_6 absorption may be readily probed at elevated temperatures in a shock tube environment.

An experimental trace of the absorption of the P(20) line by a shock-heated mixture of 0.06 percent SF_6 in Ar is shown in Figure 2. The two sharp Schlieren spikes mark the arrival of the incident and reflected shock fronts, respectively. Measurements performed later in NF_3 and NH_3 employed more refined optics and showed less of a Schlieren effect. With the exception of these spikes, the signal-to-noise ratio is very high. The decrease in absorption immediately following the reflected shock is due to dissociation of

the SF_6. The major product of the decomposition reaction is SF_4, which is not expected to absorb at 10.6 μm. The initial concentration of SF_6 is so small that the temperature and pressure remain nearly constant during dissociation.

Note that the total absorption is less behind the reflected shock even though the density is higher (indeed the absorption is highest prior to the shock). The P(20) transition at 944 cm^{-1} is near coincident with the peak of the SF_6 ν_3 bandshape at room temperature. As the temperature increases the band broadens and shifts to the red and thus the absorption decreases.[12]

Measurements similar to that shown in Figure 2 were performed for the P(20), P(24), and P(28) CO_2 laser transitions. The measured transmitted intensities were converted to absorption coefficients through use of Eq. (2). SF_6 dissociation became too rapid at temperatures exceeding 2500 K to allow evaluation of the absorption coefficient directly behind the reflected shock, i.e., prior to significant dissociation. Although not shown, both laser intensity and SF_6 concentration were varied in the present study so as to ensure the linearity of the absorption. The measured absorption coefficients versus temperature are shown in Figure 3. The temperature corresponding to peak absorption increases with decreasing frequency of the laser transition as expected.

The present results are compared with those of Nowak and Lyman[12] in Figures 3a-c. These appear to be the only other high temperature results available. The agreement between the two data sets is reasonable, however in certain temperature ranges the observed differences are outside of our measurement uncertainty of 15 percent. Part of this discrepancy may be due to the fact that the measurements of Ref. 12 were performed with a single beam system at pressures an order of magnitude below those of the present study.

The cause of the discrepancy at room temperature is not clear, however, our room temperature measurement for the P(20) transition is in agreement with earlier observations.[13]

The impact of the shock tube boundary layer flow on the uncertainty in the measured absorption coefficient must also be evaluated. In particular, SF_6 absorbs much more strongly at room temperature than at elevated temperatures, and thus the absorption contribution of the colder boundary layer region will be enhanced relative to that of the heated gas. However, at the high pressures of the present measurements, we find that less than 0.2 percent of the molecules within the optical line of sight fall within the boundary layer. This fraction is sufficiently small so that absorption within the boundary layer may be neglected.

3.2 NF_3

Measurements of absorption by NF_3 were made for the P(20) CO_2 laser line over the temperature range 300 to 2100 K at pressures of 17 to 70 atm. The mixture used was 3.0 mole percent NF_3 in Ar.

NF_3 is quite distinct from SF_6 in that its fundamental bands are centered at 906 cm^{-1} and 1032 cm^{-1},[14,15] rather than at 948 cm^{-1}. Thus the room temperature absorption coefficient of NF_3 at CO_2 laser wavelengths is quite small. With increasing temperature these fundamental bands should spread and shift towards the red, thus providing for an increased absorption coefficient at CO_2 laser wavelengths.

This is indeed borne out by experiment. A typical absorption history taken for the P(20) transition in a mixture of NF_3/Ar is shown in Figure 4. Here the absorption increases as the incident and reflected shocks pass. The

decrease in absorption observed beyond the reflected shock front is the result of chemical reaction associated with NF_3 dissociation.

The kinetics which describe NF_3 decomposition in an NF_3/Ar mix are given in Table 2 as taken from Ref. 16. Equilibrium predictions performed for the experimental conditions show complete decomposition of NF_3 above ~1000 K. Indeed the initial dissociation of NF_3 is rapid, the characteristic time for the reaction

$$NF_3 + Ar \rightarrow NF_2 + F + Ar \qquad (2)$$

is calculated to be 1 μs at T = 1500 K and P = 30 atm. Nonetheless the measured absorption coefficient remains high at these temperatures. This is because the rate of NF_2 decomposition is slower than that for NF_3 decomposition, and as soon as the NF_3 concentration drops by a factor of ~2, the reverse of reaction (2) regenerates NF_3. Furthermore, the radical NF_2 itself has absorption bands at 1074 cm^{-1} and 931 cm-1,[7,15] and can also absorb the laser radiation.

Our reflected shock measurements exhibit evidence of NF_3 decomposition at temperatures exceeding 1200 K, i.e., laser transmission increases with increasing time after shock passage, however, observed absorption decay times, even at temperatures as high as 1900 K, are many hundreds of microseconds.

The reaction mechanism shown in Table 2 has been exercised to provide kinetic predictions for comparison with the data. For the data shown in Figure 4, the NF_3 concentration is predicted to drop by a factor of three almost instantaneously at the reflected shock front, with concomitant formation of NF_2. Then the NF_3 concentration is predicted to remain essentially constant for the next several hundred microseconds while the NF_2 concentration

slowly drops, primarily due to reactions 2-4 of Table 2. Therefore, it appears that the observed absorption signal directly behind the reflected shock front is due to the sum of NF_3 and NF_2 absorptions and that the subsequent decay in absorption is primarily due to the decreasing concentration of the NF_2 radical. This behavior is typical of the data as a whole.

The measured absorption coefficients of NF_3 are presented versus temperature in Figure 5. Total pressure was varied by a factor of four at temperatures of ~1000 K with no apparent variation in the absorption coefficient, verifying that the measurements were performed in the overlapping line limit. Effects due to NF_3 decomposition were noted at temperatures above 1200 K and thus absorption coefficients are presented for three different times behind the reflected shock front The data for 5 μs corresponds to absorption prior to significant loss of (NF_3 + NF_2), but does include the effect of variations in the NF_3/NF_2 ratio. The smooth increase of the absorption coefficient (5 μs) with temperature may imply that the individual absorption coefficients of NF_3 and NF_2 are not widely dissimilar. Very rapid decomposition, directly behind the shock front, is observed at temperatures beyond ~2000 K.

It should be emphasized that the absorption data presented for temperatures above 1200 K is not fundamental but rather specific to the experimental conditions. Furthermore the data is plotted versus temperature evaluated under the assumption of frozen chemistry. NF_3 decomposition is an endothermic process and thus leads to gas cooling. For example, the kinetic calculations for the case presented in Figure 4 predict a 225 K drop in temperature directly behind the reflected shock, resulting from reaction (2). The magnitude of this temperature drop is of course directly proportional to the initial mole fraction of NF_3 in the mix.

Nonetheless these observations are valuable in demonstrating the variability that can be produced by finite rate chemistry when absorption of laser energy is used to rapidly heat a gas mixture. The potential use of absorptive species whose dissociative fragments can also absorb the laser energy is particularly interesting.

There appears to be no other measurements of CO_2 laser absorption by NF_3 for comparison with the present results. The broadband room temperature infrared absorption spectrum of NF_3 has been reported by Pace and Pierce.[14] An analysis of their spectrum yields an absorption coefficient at 10.6 μm in agreement with the present evaluation.

3.3 NH_3

Shock tube measurements of NH_3 absorption coefficients were made using two different gas mixtures: 9.4 percent NH_3 in Ar, studied over the temperature range 900 to 2300 K at 10 to 40 atm pressure, and 5 percent NH_3, 45% H_2, and 50 percent Ar studied over the temperature range 900 to 2900 K at 5 to 16 atm. The absorption measurements were made for the P(20) 10.6 μm CO_2 line which falls in the valley between the peaks of the split NH_3 ν_2 band at 932 and 965 cm^{-1}. Therefore an initial increase in absorption is expected as the temperature increases and the band fills in.

A typical experimental absorption trace in a mix of 9.4 percent NH_3 in Ar is shown in Figure 6. The large spike at 240 ns is caused by the firing of a pulsed CO_2 laser which was timed to trigger 80 μs after the reflected shock. The pulsed laser was used as part of a separate experiment to study potential absorption saturation in NH_3; the saturation work has been discussed earlier[8] and is not presented here.

It can be seen in Figure 6 that there is a large increase in absorption after passage of the incident shock and an additional increase after reflected shock passage. It must be noted that the room temperature ν_2 absorption spectra will be quite structured at the preshock pressures near 1 atm with the spacing between strong lines in some spectral regions being large compared to the line width.[18] Thus the observed preshock absorption coefficient may depend on total pressure as well as absorber concentration. This point has been discussed by Patty et al.[19] who present measurements of atmospheric pressure, room temperature NH_3 absorption coefficients at CO_2 laser wavelengths. The NH_3 spectra becomes richer at the elevated temperatures and pressures behind the shock and there is sufficient overlap between adjacent lines so that the measured absorption coefficients are to first order independent of total pressure. This observation was verified over a factor of four in pressure in the present measurements at temperatures near 1000 K.

Referring again to Figure 6, it can be seen that the absorption trace is approximately constant behind the incident shock but decreases steadily behind the reflected shock. This decrease can be directly related to chemical relaxation. The decomposition kinetics of NH_3 and its fragments are well established and the relevant chemical reactions and rate constants are listed in Table 3 as taken from Refs. 20 and 21.

As was the case with NF_3 the observed decrease in absorption is much slower than the characteristic decomposition time evaluated from the reaction

$$NH_3 + Ar \rightarrow NH_2 + H + Ar \quad . \tag{3}$$

For the conditions of Figure 6, P = 34.1 atm, T = 2315 K, the characteristic relaxation time for reaction (3) would be ~10 μs. The reason for this

discrepancy is twofold: 1) upon modest dissociation the reverse of reaction (3) becomes important and 2) the gas cooling caused by the endothermic decomposition of NH_3 acts to slow down the chemistry.

The kinetic model of Table 3 has been exercised for the test conditions and in all cases the predicted concentration of NH_3 tracked the measured absorption trace quite well. This was expected both because the kinetic mechanism is well established (and in general is deduced from global measurements of NH_3 decay in shock tubes), and the NH_3 dissociation fragments do not provide for significant absorption at CO_2 laser wavelengths.

Measured absorption coefficients for the 9.4 percent NH_3 data are shown plotted versus temperature in Figure 7. In this case the temperature plotted is that deduced from the kinetic calculations, which is only different from the "frozen chemistry" temperature at the highest temperature shown. This latter data point has also been corrected for the predicted decrease in NH_3 concentration. As can be seen, the absorption coefficient is relatively constant between 800 to 2200 K. Measurements in NH_3-Ar mixtures could not be performed at higher temperatures because of rapid NH_3 decomposition.

The kinetic predictions showed that reaction (2) of Table 3 provides the rate limiting step for NH_3 decomposition and indicated therefore that if H_2 were added to the gas mix the rate of NH_3 decomposition would decrease. The opposite effect would occur upon H_2 addition to the SF_6 and NF_3 mixes due to the formation of HF. Therefore, a series of measurements were performed in a mix of 5 percent NH_3/45 percent H_2/50 percent Ar, since H_2 is the diluent of choice for the laser propulsion application.

A typical absorption history for this mixture is shown in Figure 8. Once again the spike observed in the signal shortly after passage of the reflected

shock is due to the pulsed CO_2 laser used in the saturation experiment and may be ignored in the present analysis. Although the reflected shock temperature of this measurement is similar to that of the data presented in Figure 6, no NH_3 decomposition is evident. This observation is in complete accord with the chemical kinetic predictions and reflects the role H_2 plays in reforming NH_3. With this mixture, absorption measurements could be performed at temperatures up to 2900 K before NH_3 decomposition compromised the measurement. The measured absorption coefficients for this gas mix are also presented in Figure 7 and are in good agreement with those from the NH_3/Ar mixture.

The only other published measurement for CO_2 laser absorption by NH_3 at elevated temperature is that by Fowler.[22] Unfortunately it is difficult to specify the chemical and vibrational states of the gas in these experiments and therefore those measurements cannot be compared directly to the present observations.

4. SUMMARY

The high pressure (overlapping line) absorption coefficients of SF_6, NF_3, and NH_3 for the P(20) CO_2 laser line have been measured over the temperature range of 300 to 2900 K. In the case of SF_6, measurements were also provided for the P(24) and P(28) transitions of the CO_2 laser. It has been demonstrated that even at the high pressures of the current experiments, P = 1[illegible] to 7[illegible] atm, molecular absorption can be prolonged at temperatures well above those suggested by equilibrium gas constraints under conditions of rapid gas heating through the mediation of finite rate chemistry. Furthermore, additional absorption can be provided by the dissociation fragments of less stable seed molecules. Both observations are important considerations in

applications where rapid gas heating by lasers is desirable, such as laser propulsion.

A summary plot of the present observations, along with earlier data[7] for H_2O, is given in Figure 9. The absorption coefficients shown here are normalized by mass rather than number density to illustrate the relative efficiency for seeding a hydrogen-based propellant system. It can be seen that seeding with small quantities of absorbing gases such as NH_3 and H_2O can provide efficient and continuous absorption of CO_2 laser radiation from room temperature to temperatures in excess of 3500 K.

ACKNOWLEDGEMENTS

This work was sponsored by the Air Force Office of Scientific Research under Contract F49620-83-C-0039 monitored by Dr. Len Caveny.

References

1. A. Kantrowitz, "Propulsion to Orbit by Ground-Based Laser," Astronautics and Aeronautics, V. 10, No. 5, May 1972, p. 74.

2. R.F. Weiss, A.N. Pirri, and N.H. Kemp, "Laser Propulsion," Astronautics and Aeronautics, March 2, 1979, p. 50.

3. N.H. Kemp, D.I. Rosen, and H.H. Legner, "Laser Energy Absorption in Gases: Research Problems," Orbit-Raising and Maneuvering Propulsion: Research Status and Needs, AIAA Progress in Astronautics and Aeronautics, Vol. 89, edited by Leonard H. Caveny, AIAA, New York, p. 73.

4. D.I. Rosen, A.N. Pirri, R.F. Weiss, and N.H. Kemp, "Repetitively Pulsed Laser Propulsion: Needed Research," L.H. Caveney, op. cit. p. 95.

5. N.H. Kemp and H.H. Legner, "Steady (Continuous Wave) Laser Propulsion: Research Areas," L. H. Caveny, op. cit. p. 109.

6. G.E. Caledonia, "Conversion of Laser Energy to Gas Kinetic Energy," J. of Energy 1, p. 121-124, (1977).

7. E. Pugh and R.H. Krech, "Absorptivity of Water Vapor for 10.6 μm Radiation," AIAA J. 20, (1982).

8. R.H. Krech, L.M. Cowles, G.E. Caledonia, and D.I. Rosen, "Linear and Non-linear Absorption of Hot SF_6 and NH_3 at 10.6 μm," Proceedings of the 15th International Symposium on Shock Tubes and Waves, Berkeley, CA (1985), to be published.

9. E.F. Green and J.P. Toennes, "Chemical Reaction in Shock Waves," Arnold, London (1964).

10. J.F. Bott and T.A. Jacobs, "Shock-Tube Studies of Sulfur Hexafluoride," J. Chem. Phys. 30, 3850 (1969).

11. K.L. Wray and E.V. Feldman, "The Pyrolysis and Subsequent Oxidation of SF_6," Proceedings of the 14th Symposium on Combustion, Combustion Institute (1973), pp. 229-240.

12. A.V. Nowak and J. Lyman, "The Temperature-Dependent Absorption Spectrum of the ν_3 Band of SF_6 at 10.6 μm," J. Quant. Spectrosc. Radiat. Transf. 15, 945 (1975).

13. J.D. Anderson, Jr., J.L. Wagner, and J. Knott, "CO_2 Laser Radiation Absorption in SF_6-Air Mixtures," AIAA J. 11, 1424 (1973).

14. E.L. Pace and L. Pierce, "Infrared and Raman Spectra of Nitrogen Trifluoride," J. Chem. Phys. 23, 1248 (1951).

15. JANAF Thermochemical Tables, second edition, ed. D.R. Stull and H. Prophet, NSRDS-NBS 37, U.S. Dept. of Commerce (June 1971).

16. D.L. Baulch, J. Duxbury, S.J. Grant, and D.C. Montague, "Evaluated Kinetic Data for High Temperature Reactions, Vol. 4, Homogeneous Gas Phase Reactions of Halogen-and Cyanide-Containing Species," J. Phys. Chem. Ref. Data 10, Suppl. 1 (1981).

17. M.D. Harmony and R.J. Myers, "Infrared Spectrum and Thermodynamic Functions of the NF_2 Radical," J. Chem. Phys. 37, 636 (1962).

18. F.W. Taylor, "Spectral Data for the ν_2 Bands of Ammonia with Applications to Radiative Transfer in the Atmosphere of Jupiter," J. Quant. Spectrosc. Radiat. Transfer 13, 1181 (1973).

19. R.R. Patty, C.M. Russworn, W.A. McClenny, and D.R. Morgan, "CO_2 Laser Absorption Coefficients for Determining Ambient Levels of O_3, NH_3, and C_2H_4," Appl. Opt. 13, 2850 (1974).

20. D.L. Baulch, J. Duxbury, S.J. Grant, and D.C. Montague, "Evaluated Kinetic Data for High Temperature Reactions," Vol. 2, Buttersworth, London-Boston (1975).

21. R.C. Flagen, S. Galant, and J.P. Appleton, "Rate Constrained Particle Equilibrium Models for the Formation of Nitric Oxide From Organic Fuel Nitrogen," Comb. and Flame 22, 299 (1974).

22. M.C. Fowler, "Measured Molecular Absorptivities for a Laser Thruster," AIAA J. 19, 1009 (1981).

Table 1. Parameter Range of Absorption Measurements

SF_6 (6×10^{-2}% in Ar)
P = 10 to 70 atm
T = 500 to 2500 K
P(20), P(24), P(28) lines
NF_3 (3% in Ar)
P = 17 to 70 atm
T = 500 to 2100 K
P(20) line
NH_3 (9.4% in Ar, 5% in H_2/Ar)
P = 5 to 40 atm
T = 900 to 2900 K
P(20) line

Table 2. NF_3 Kinetics

Reaction	Rate Constant, cm^3/s (Ref. 15)
1. $NF_3 + Ar \rightarrow NF_2 + F + Ar$	$6.8 \times 10^{-8} e^{-24160/T}$
2. $NF_2 + Ar \rightarrow NF + F + Ar$	$1.3 \times 10^{-9} e^{-25700/T}$
3. $NF_2 + F_2 \rightarrow NF_3 + F$	$8 \times 10^{-12} e^{-7300/T}$
4. $NF + NF \rightarrow N_2 + 2F$	4×10^{-11}
5. $NF_2 + NF_2 \rightarrow NF_3 + NF$	$8 \times 10^{-13} e^{-18600/T}$
6. $F_2 + Ar \rightarrow 2F + Ar$	$3.5 \times 10^{-11} e^{-16970/T}$

Table 3. Ammonia Decomposition Kinetics

Reaction	Rate Constants (cm^3/s, cm^6/s)
1. $NH_3 + Ar \leftrightarrow NH_2 + H + Ar$	$1.5 \times 10^{-8}\ e^{-42400/T}$
2. $H + NH_3 \leftrightarrow NH_2 + H_2$	$4.6 \times 10^{-11}\ e^{-8700/T}$
3. $NH_2 + H \leftrightarrow NH + H_2$	$1.7 \times 10^{-13} T^{.67}\ e^{-2150/T}$
4. $NH_2 + NH_2 \leftrightarrow NH_3 + NH$	$9.6 \times 10^{-11}\ e^{-1800/T}$
5. $NH + N \leftrightarrow N_2 + H$	1.7×10^{-11}
6. $NH + H \leftrightarrow N + H_2$	$1.7 \times 10^{-12}\ T^{.68}\ e^{-960/T}$
7. $N + N + M \leftrightarrow N_2 + M$	$8.3 \times 10^{-34}\ e^{500/T}$
8. $H + H + M \leftrightarrow H_2 + M$	$2 \times 10^{-30}\ T^{-1}$

Figure 1. Schematic of optical arrangement for low intensity absorption measurements

Figure 2. Typical absorption history in an SF_6/Ar mixture P(20) CO_2 laser transition

Figure 3a. High pressure SF_6 CO_2 laser absorption coefficient versus temperature. P(20) transition (symbols are present results, solid lines are from Ref. 12)

Figure 3b. High pressure SF_6 CO_2 laser absorption coefficient versus temperature. P(24) transition (symbols are present results, solid lines are from Ref. 12)

Figure 3c. High pressure SF_6 CO_2 laser absorption coefficient versus temperature. P(28) transition (symbols are present results, solid lines are from Ref. 12)

Figure 4. Typical absorption signal history in NF_3/Ar test. P(20) CO_2 laser transition. T_5 is the frozen shock temperature, with no dissociation.

Figure 5. Measured NF_3 absorption coefficients for the CO_2 P(20) laser transition for several times after reflected shock passage (based on frozen jump condition density and temperature), 3% NF_3 in Argon

Figure 6. Typical absorption trace in NH_3/Ar test

Figure 7. Measured high pressure absorption coefficients for NH_3 at the P(20) CO_2 laser transition for two gas mixes

Figure 8. Typical absorption trace in NH_3/H_2/Ar test, P(20) transition

Figure 9. Experimental high pressure absorption coefficients versus temperature

EXPERIMENTAL SET-UP FOR SHOCK TUBE ABSORPTION MEASUREMENTS

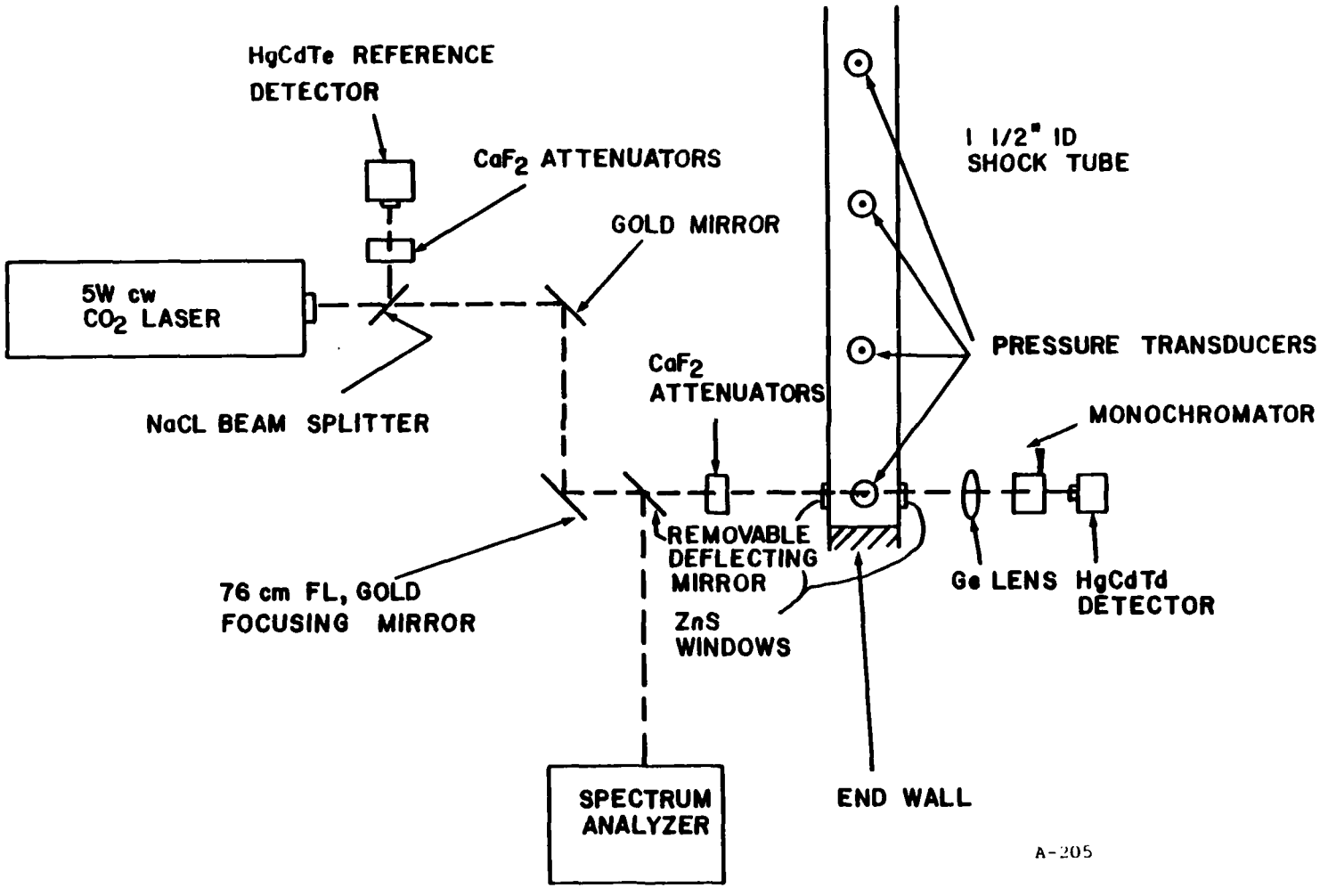

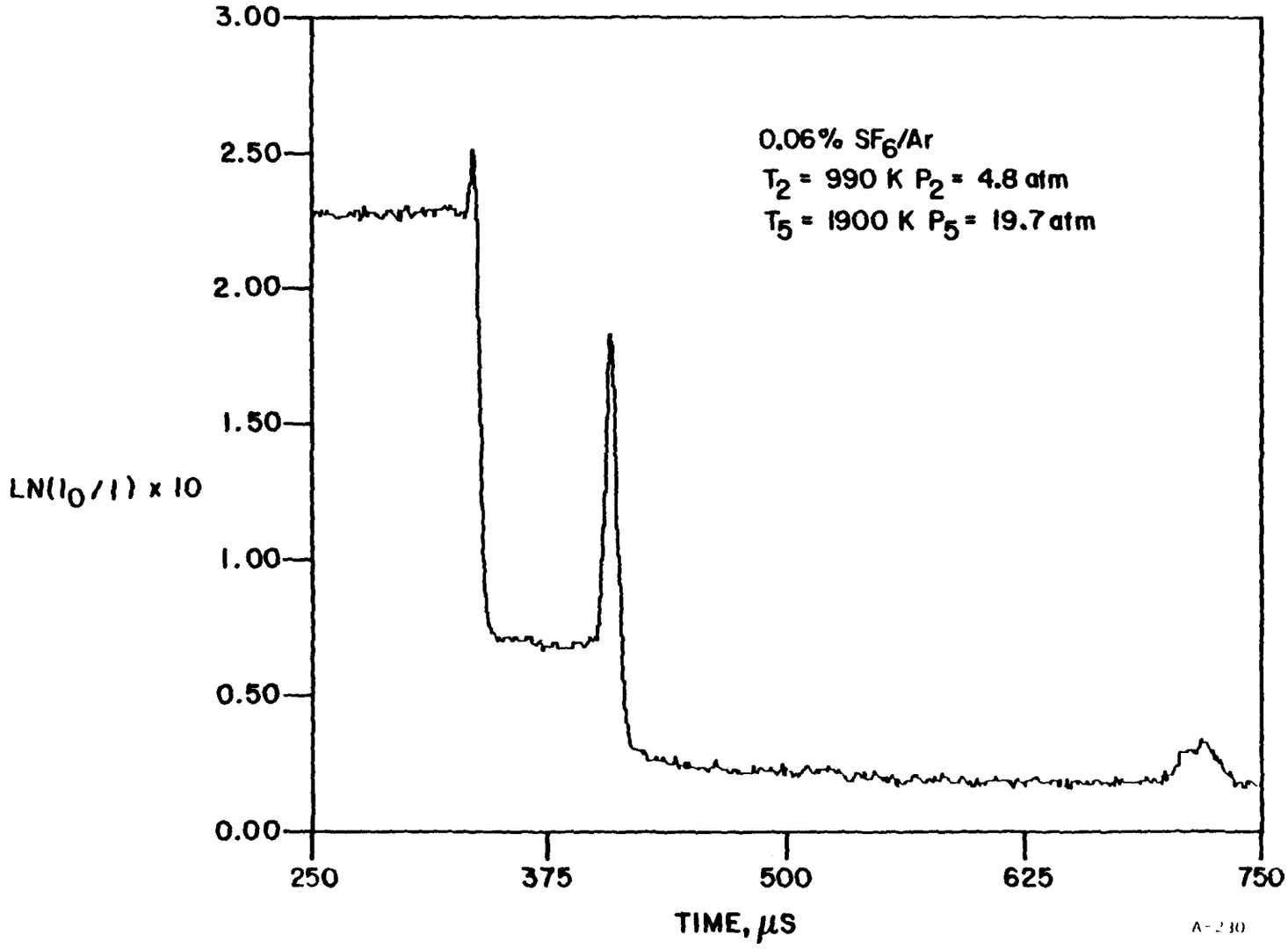
0.06% SF_6/Ar
T_2 = 990 K P_2 = 4.8 atm
T_5 = 1900 K P_5 = 19.7 atm
LN(I_0/I) x 10
3.00
2.50
2.00
1.50
1.00
0.50
0.00
250
375
500
625
750
TIME, μS
A-230

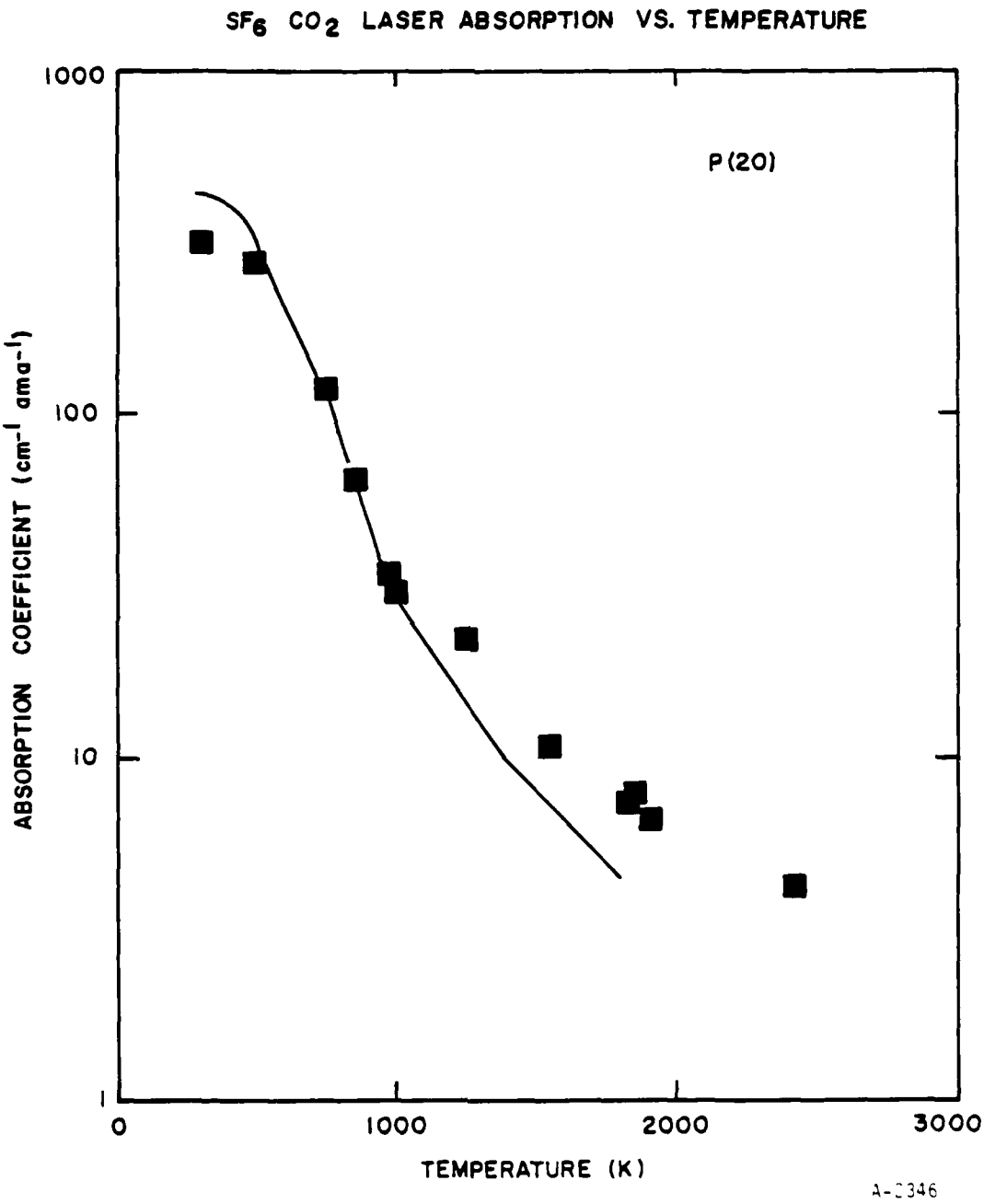
SF6 CO2 LASER ABSORPTION VS. TEMPERATURE
P(20)
ABSORPTION COEFFICIENT (cm-1 ama-1)
1000
100
10
1
0
1000
2000
3000
TEMPERATURE (K)
A-2346

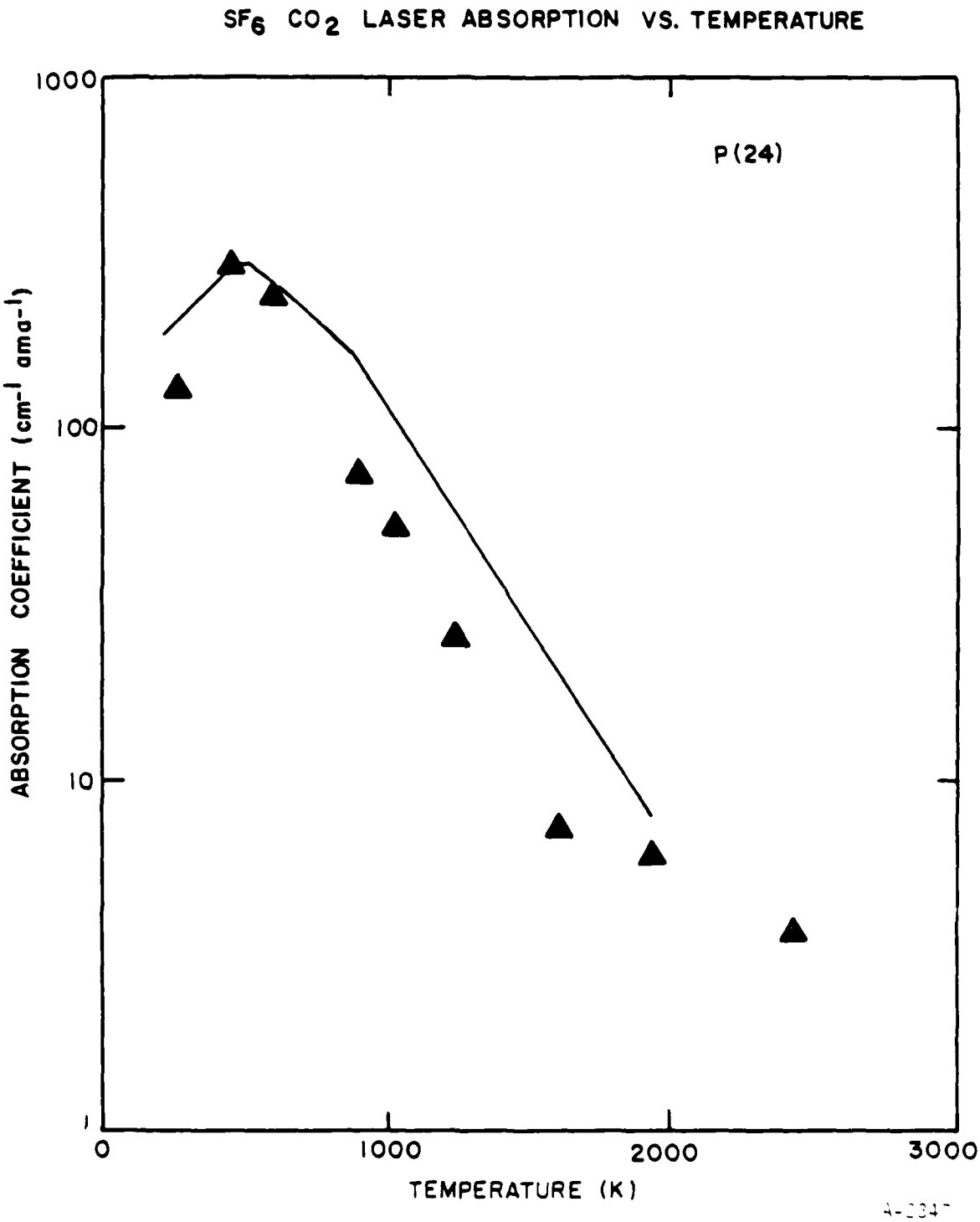
SF6 CO2 LASER ABSORPTION VS. TEMPERATURE
P(24)
ABSORPTION COEFFICIENT (cm-1 atma-1)
1000
100
10
1
0
1000
2000
3000
TEMPERATURE (K)
A-2347

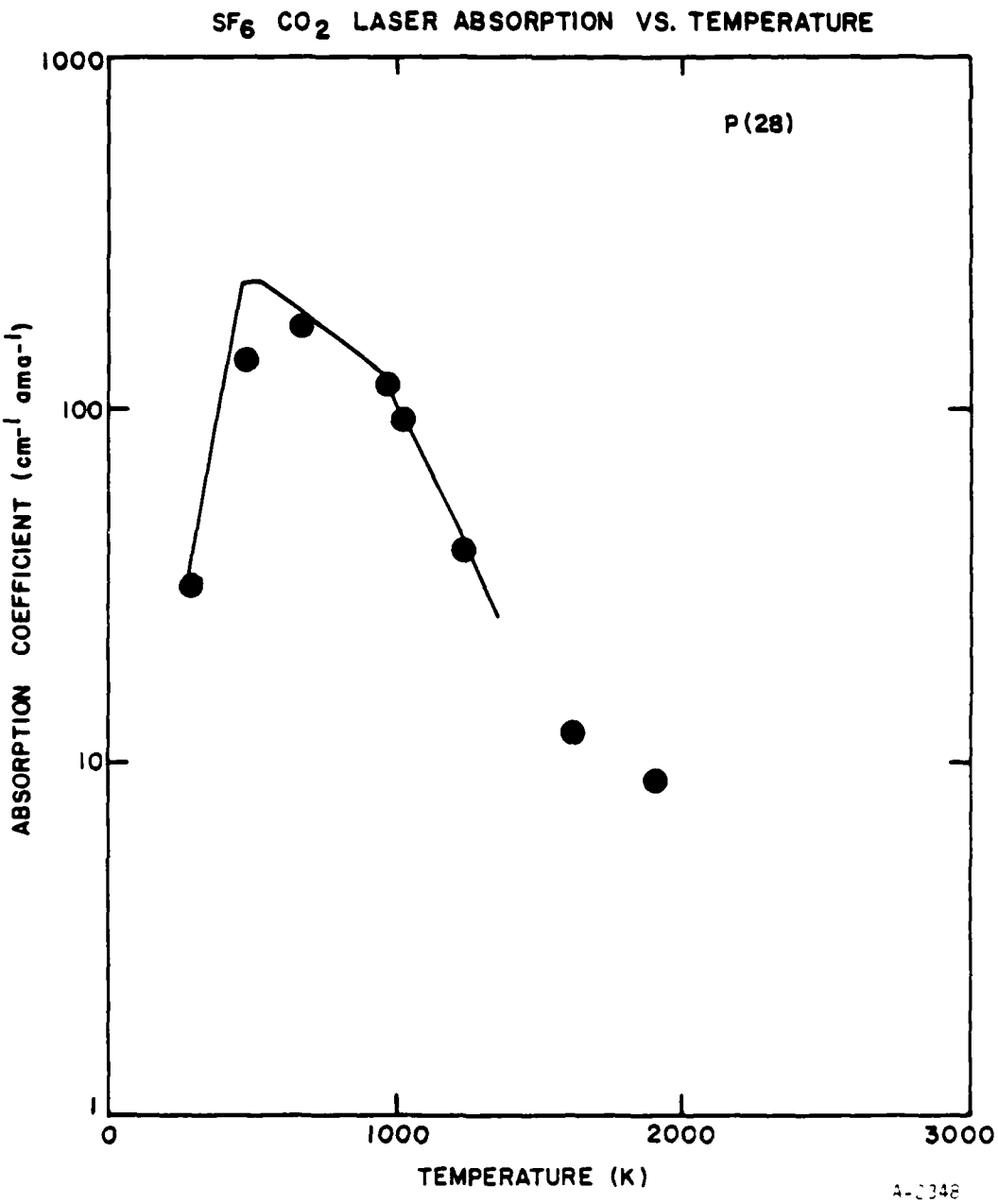
SF6 CO2 LASER ABSORPTION VS. TEMPERATURE
P(28)
ABSORPTION COEFFICIENT (cm-1 atm-1)
1000
100
10
1
0
1000
2000
3000
TEMPERATURE (K)
A-0348

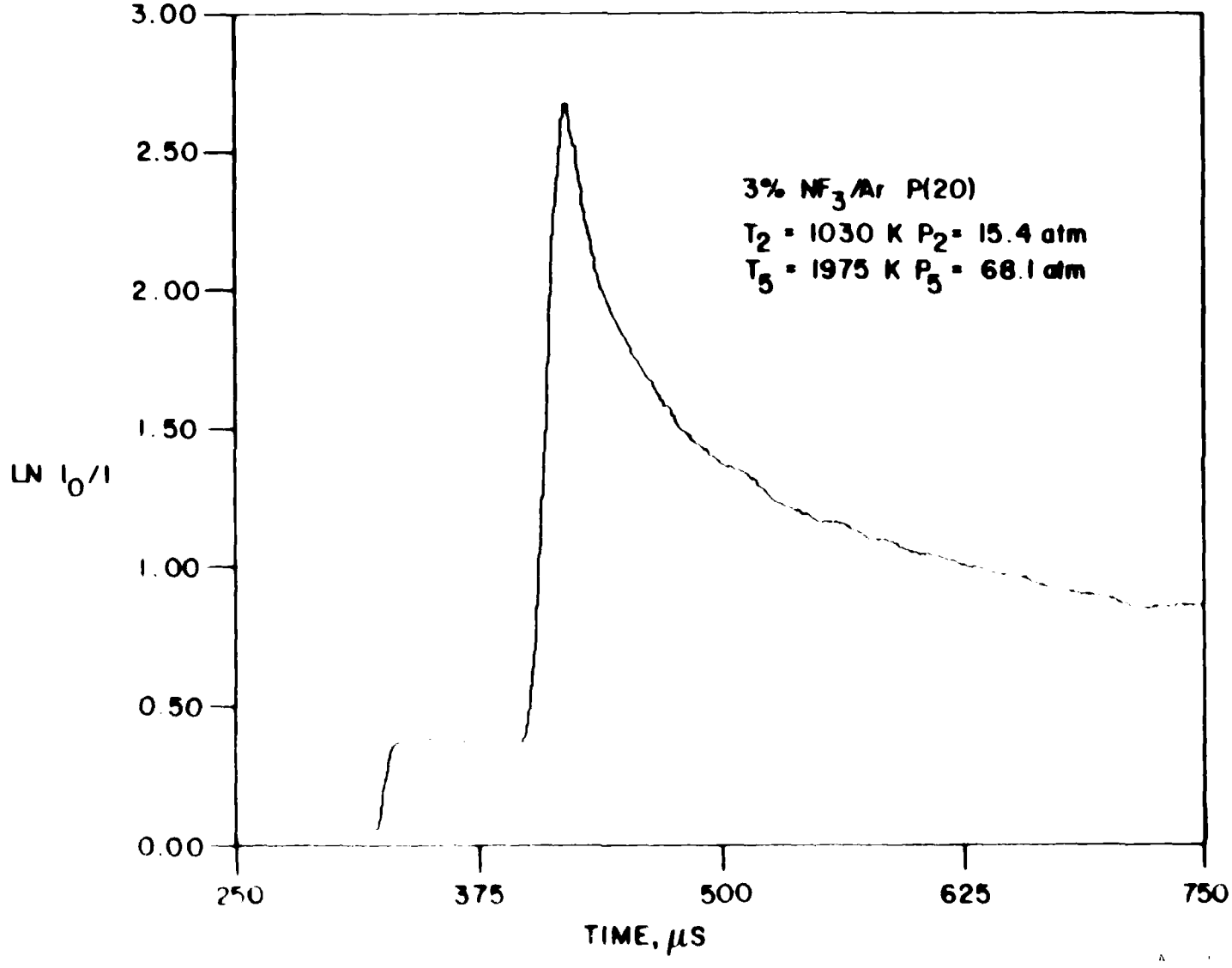
3% NF_3/Ar P(20)
T_2 = 1030 K P_2 = 15.4 atm
T_5 = 1975 K P_5 = 68.1 atm
LN I_0/I
3.00
2.50
2.00
1.50
1.00
0.50
0.00
250
375
500
625
750
TIME, μS

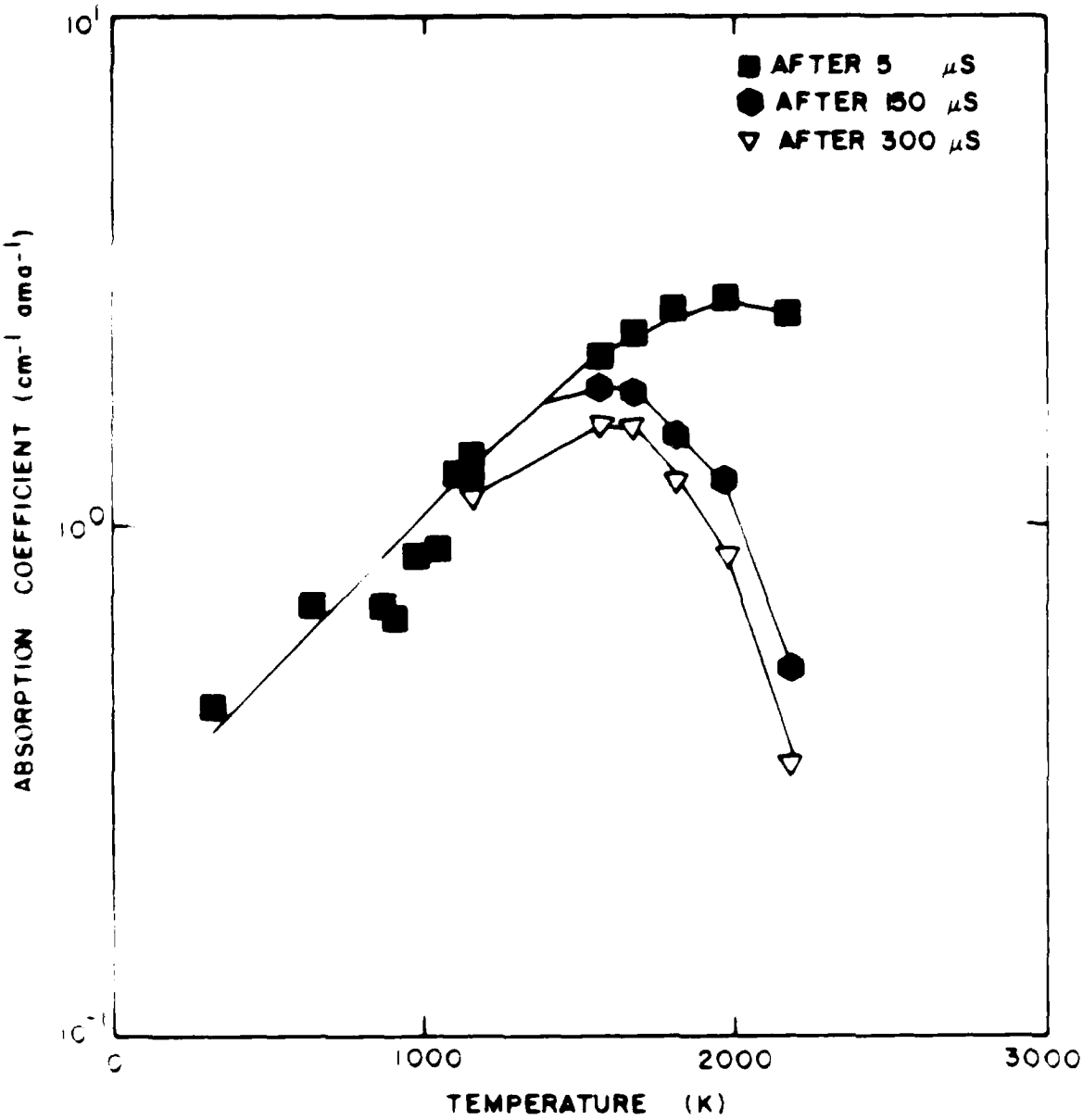
AFTER 5 μS
AFTER 150 μS
AFTER 300 μS
ABSORPTION COEFFICIENT (cm⁻¹ amg⁻¹)
10¹
10⁰
10⁻¹
0
1000
2000
3000
TEMPERATURE (K)

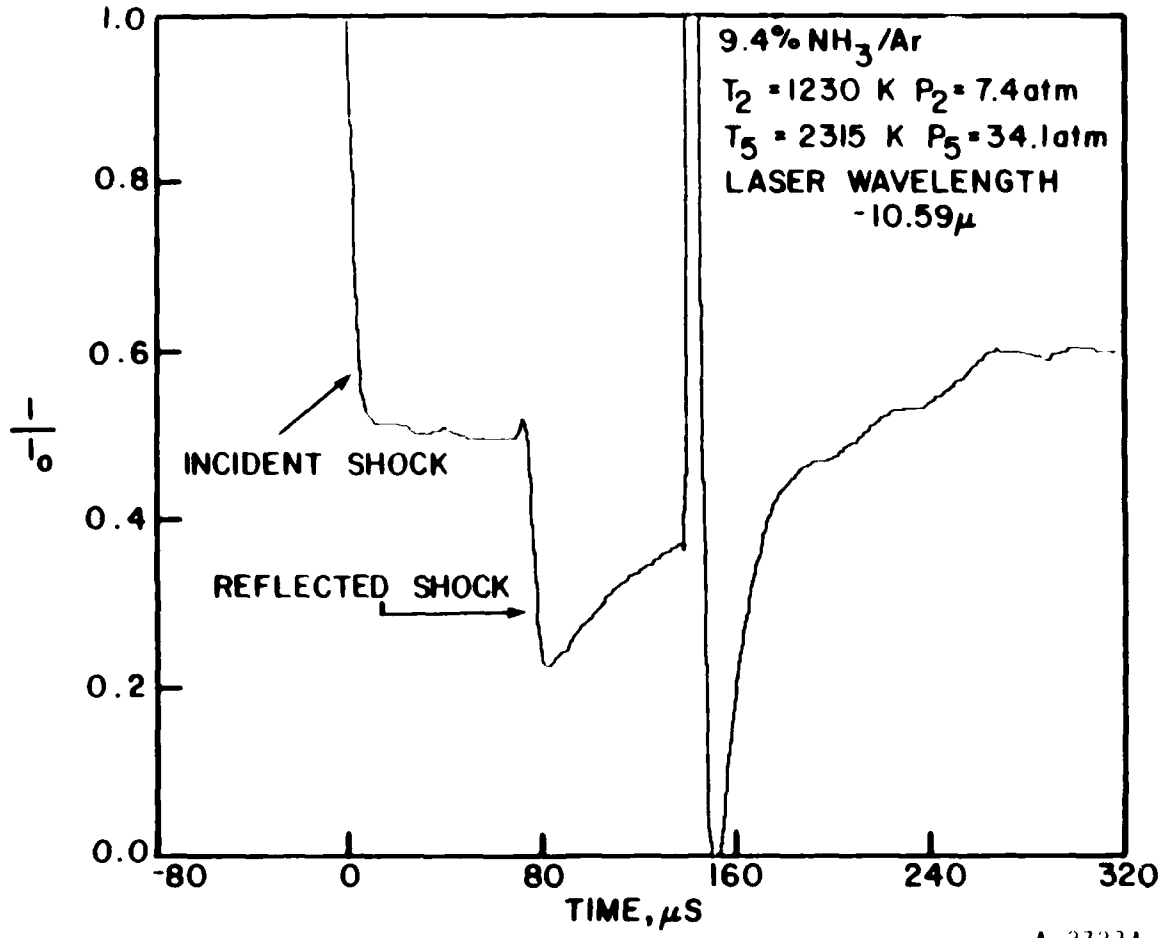
9.4% NH_3/Ar
T_2 = 1230 K P_2 = 7.4 atm
T_5 = 2315 K P_5 = 34.1 atm
LASER WAVELENGTH
~10.59μ
INCIDENT SHOCK
REFLECTED SHOCK
$\frac{I}{I_0}$
1.0
0.8
0.6
0.4
0.2
0.0
-80
0
80
160
240
320
TIME, μS
A-2723L

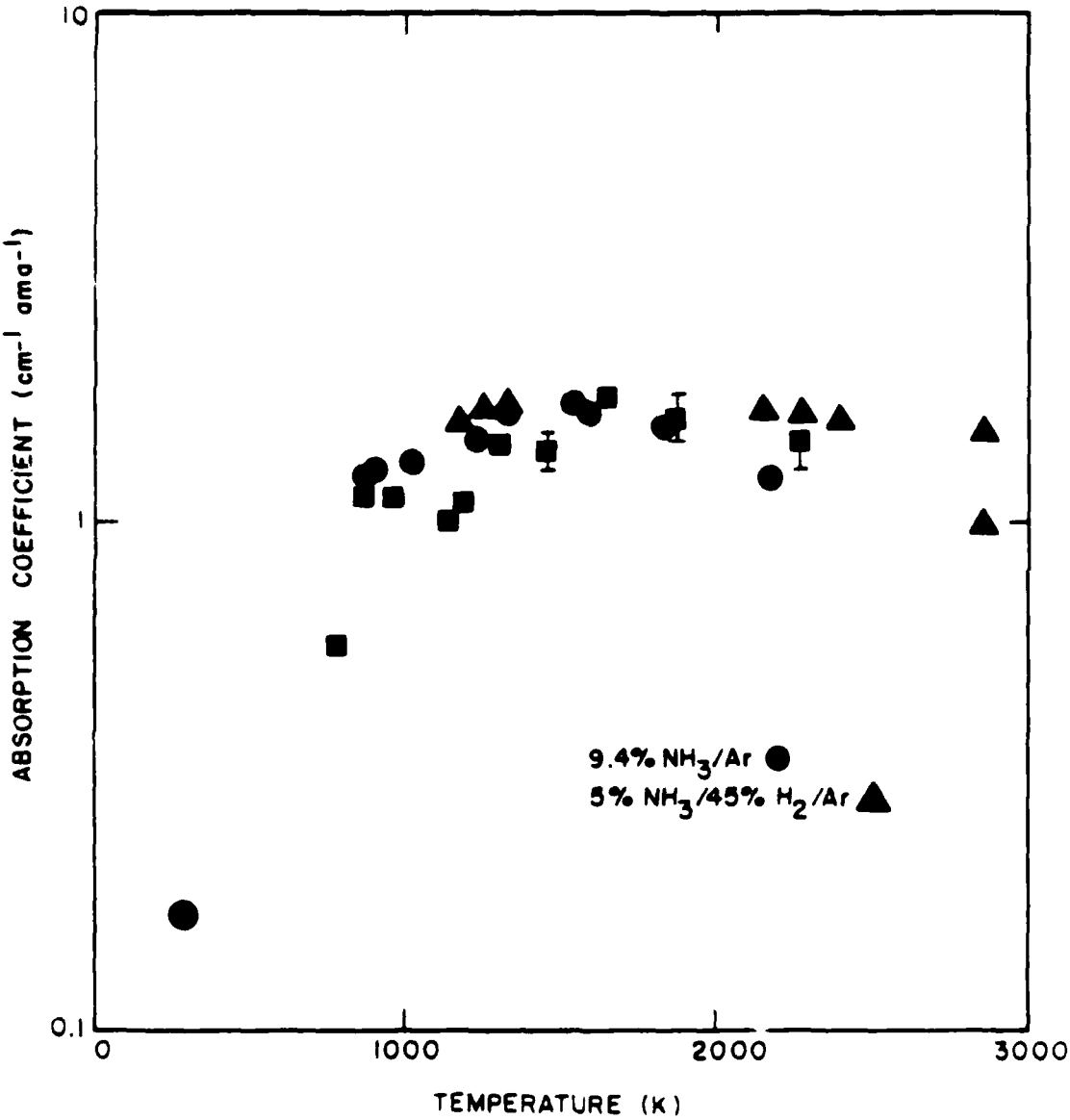
10
1
0.1
0
1000
2000
3000
ABSORPTION COEFFICIENT (cm⁻¹ amg⁻¹)
TEMPERATURE (K)
9.4% NH3/Ar
5% NH3/45% H2/Ar

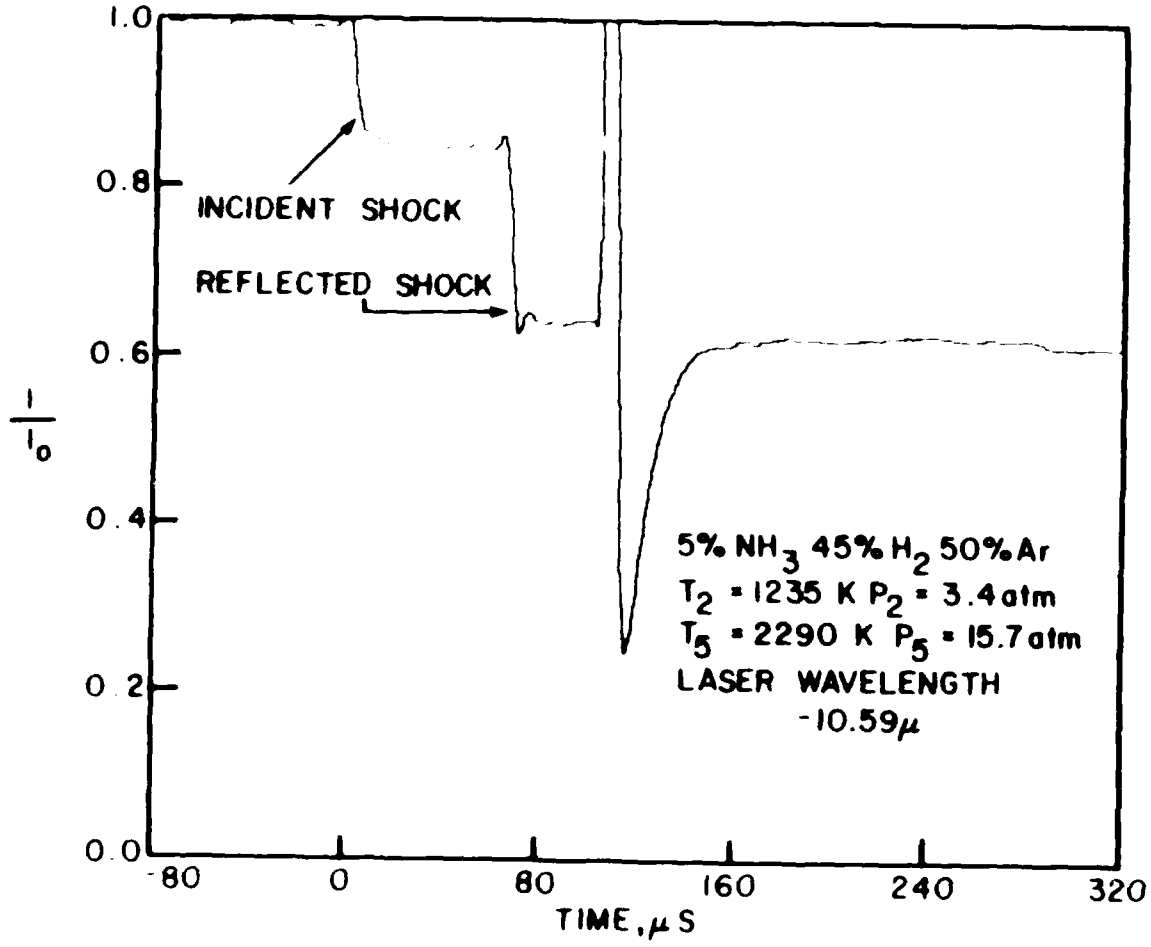
1.0
0.8
0.6
0.4
0.2
0.0
I/I0
INCIDENT SHOCK
REFLECTED SHOCK
5% NH3 45% H2 50% Ar
T2 = 1235 K P2 = 3.4 atm
T5 = 2290 K P5 = 15.7 atm
LASER WAVELENGTH
-10.59μ
-80
0
80
160
240
320
TIME, μS

A 2724 L

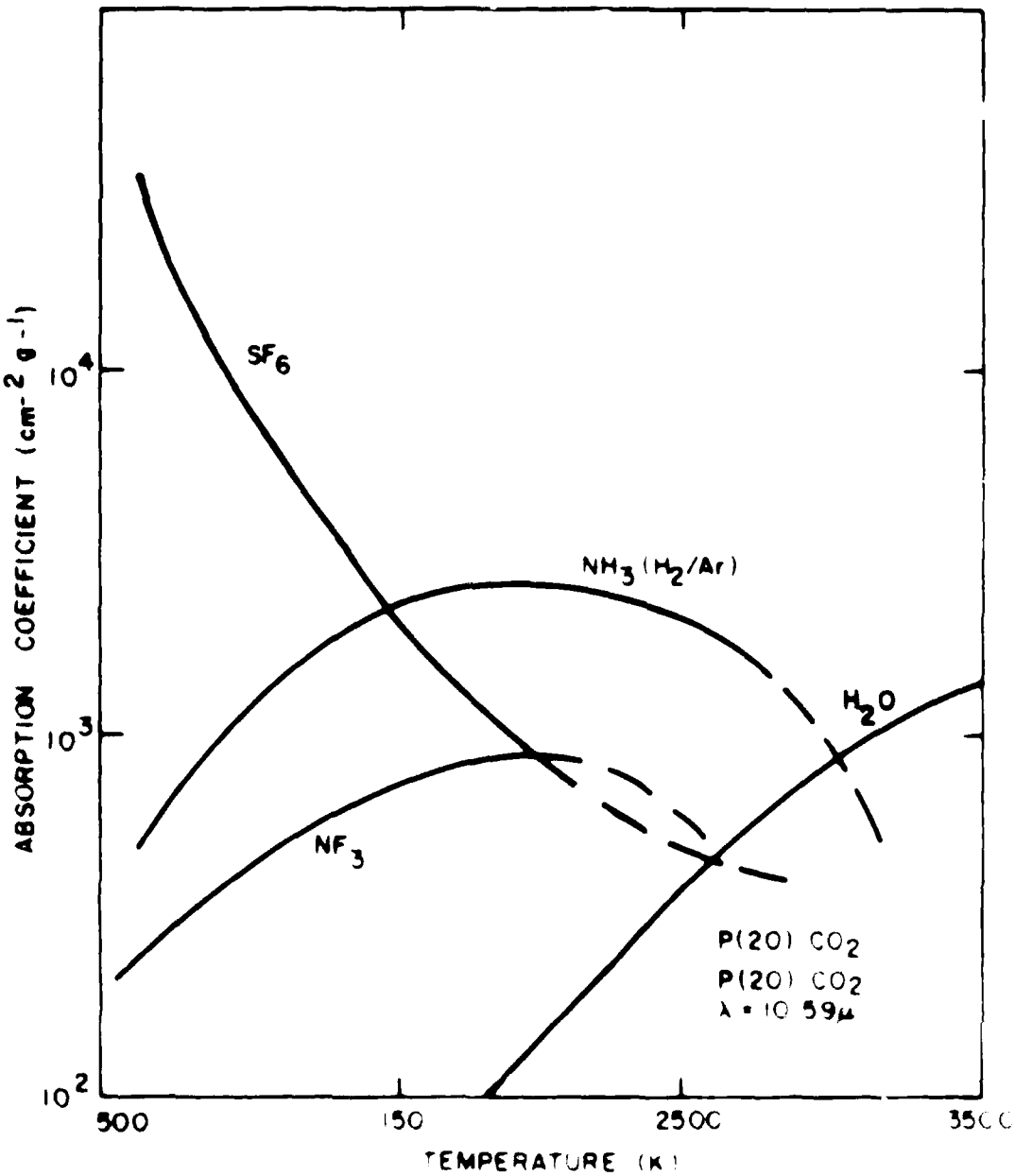
ABSORPTION COEFFICIENT (cm^{-2} g^{-1})
10^4
10^3
10^2
SF_6
NH_3 (H_2/Ar)
H_2O
NF_3
P(20) CO_2
P(20) CO_2
λ = 10.59μ
500
150
2500
3500
TEMPERATURE (K)

END

3-87

DTIC